Geological Quarterly, 2025, 69, 44
DOI: https://doi.org/10.7306/gq.1817

Gold of mesothermal Fe-Ni-Co-Bi-As type in alluvial deposits of the Wierzbiak River (Fore-Sudetic Block, SW Poland)

Marcin KANIA[1, *]

[1] Polish Geological Institute – National Research Institute, al. Jaworowa 19, Wrocław, Poland; ORCID: 0000-0002-6829-1663

Kania, M., 2025. Gold of mesothermal Fe-Ni-Co-Bi-As type in alluvial deposits of the Wierzbiak River (Fore-Sudetic Block, SW Poland). Geological Quarterly, 69, 44; https://doi.org/10.7306/gq.1817

Associate Editor: Tomasz Bajda

Study of detrital gold grains from modern sediments in the bed of the Wierzbiak River in Lower Silesia (SW Poland) provided insights into their morphological and chemical characteristics. The gold grains exhibit low shape diversity and a high degree of edge rounding. Chemically, the gold grains are homogeneous, consisting of native gold with a maximum silver content of up to 20 wt.%. The grains analysed also contain micro-inclusions, mainly composed of Ni-Co-Fe sulpharsenides and sulphides, such as pyrite, chalcopyrite, galena and native bismuth, pointing to an association of mesothermal Fe-Ni-Co-Bi-As mineralization type. The mineral inclusions observed are not typical for the quartz veins of the Wądroże Wielkie Massif but resemble the mineralization present in the polymetallic veins of the Kaczawa Metamorphic Complex. The results of this study support a thesis of a complex genesis of the local Lower Silesian gold-bearing Cenozoic placers, involving both the weathering of local quartz veins of the Wądroże Wielkie Massif and potential contributions from other ore sources in the region. Further geophysical and borehole studies are needed to more accurately assess the gold resources in the Fore-Sudetic Block, especially in the watersheds of the Wierzbiak and Nysa Szalona rivers.

Key words: gold, placer deposits, Fore-Sudetic Block, Wądroże Wielkie Massif, inclusions.

INTRODUCTION

Ore mineral micro-inclusions in gold grains found in alluvial sediments of the Sudetes rivers serve as key indicators of the crystallization conditions of gold-bearing paragenesis. Combined with analyses of grain morphology and chemical composition, they provide crucial information for determining the original source of the gold. To date, the presence of micro-inclusions has been documented and identified in gold grains collected from river sediments of the Jamna Creek near Wleń, draining the Wleń Graben (Kania, 2018) and of tributaries of the Bóbr and Kaczawa rivers eroding the deposits of the North Sudetic Depression's cover (Kania, 2023; Kania and Muszer, 2024). The micro-inclusions identified are characteristic of the local Permian red-bed successions and As-polymetallic quartz veins of the Kaczawa Metamorphic Complex (Fig. 1).

This article describes the results of studies on detrital gold from sediments in the bed of the Wierzbiak River, which flows through the Sudetes Foothills in the area of the Wądroże Wielkie Massif. A local kaolin cover developed on the gneiss outcrop, along with surrounding colluvial and alluvial deposits, was historically mined, with intense activity beginning in the 14th century and continuing intermittently until the late 19th century (Domaszewska, 1964; Grodzicki, 1966, 1972; Dziekoński, 1972; Maciejak, 2011a, b). Petrographic analyses of local Cenozoic placer deposits, as well as morphological and chemical studies of the gold grains, have suggested that Carboniferous quartz veins intersecting the Wądroże Wielkie crystalline Massif are the primary source of the local detrital gold (Grodzicki, 1966, 1972, 1998, and references therein; Banaś et al., 1985; Mikulski and Wierchowiec, 2013; Wierchowiec et al., 2018).

This study tests those earlier assumptions by searching for and identifying micro-inclusions within gold grains, particularly those inclusions consisting of ore minerals. Since the 1990s, this approach has been successfully employed to complement traditional panning methods in the exploration of Au-polymetallic primary deposits (see Leake et al., 1995; Styles, 1995; Chapman et al., 2002, 2021, 2023; Pitfield et al., 2009). A population of gold grains was recovered from contemporary channel-fill sediments of the Wierzbiak River, which drains the Wądroże Wielkie Massif that lies to the north and east. They contained numerous mineralogically diverse micro-inclusions, representing a paragenesis distinct from that found in the quartz veins of the Wądroże Massif.

These findings provide new insights into the formation of Cenozoic gold-bearing deposits in the Sudetes Foothills, highlighting their complex, polygenetic origins. Furthermore, the results support the hypothesis that local contemporary gold-bear-

* E-mail: marcin.kania@pgi.gov.pl

Received: April 15, 2025; accepted: October 14, 2025; first published online: November 28, 2025

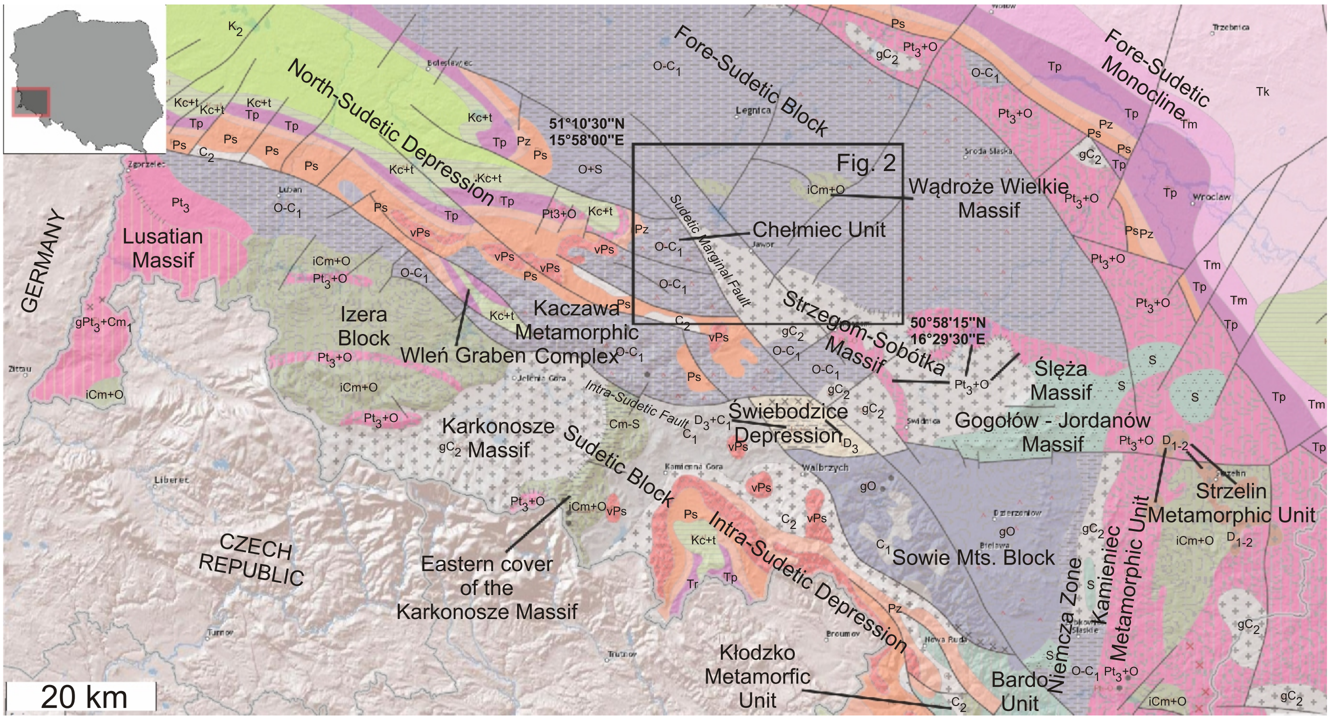

Fig. 1. Generalized geological map of the north-western part of the Lower Silesian Block, without Cenozoic cover (GeoLOG; Dadlez et al., 2000, modified)

Pt_3 – Upper Proterozoic; gPt_3+Cm_1 – Upper Proterozoic and Lower Cambrian, granitoids; Pt_3+O – Upper Proterozoic – Ordovician; iCm+O – Cambrian and Ordovician, igneous rocks; Cm-S – Cambrian – Silurian; gO – Ordovician, igneous rocks; O+S – Ordovician and Silurian; O-C1 – Ordovician – Lower Carboniferous; S – Silurian; D_{1+2} – Lower and Middle Devonian; D_3 – Upper Devonian; D_3+C_1 – Upper Devonian and Lower Carboniferous; C_1 – Lower Carboniferous; C_2 – Upper Carboniferous; gC_2 – Upper Carboniferous, granitoids; Ps – Rotliegend; vPs – Lower Permian (Rotliegend volcanic rocks); Pz – Zechstein; Tr – Triassic; Tp – Lower Triassic (Buntsandstein); Tm – Middle Triassic (Muschelkalk); Tk – Upper Triassic (Keuper); Kc+t – Upper Cretaceous (Cenomanian and Turonian). The GPS coordinates marked on the Map define the NW and SE corners of the area presented in Figure 2

ing sediments also contain gold reworked from older Cenozoic deposits, including material eroded from the crystalline basement of the Kaczawa Metamorphic Complex (Mikulski and Wierchowiec, 2013).

The research presented in this paper was possible thanks to the use of a combination of reflected light microscopic analyses, scanning electron microscopy (SEM) and *energy-dispersive X-ray spectroscopy* (EDS). SEM is commonly used in contemporary research on detrital gold: in the *secondary electron* (SE) mode for imaging grain morphology (Townley et al., 2003; Wierchowiec et al., 2018) and in the *backscattered electrons* (BSE) mode for distinguishing phases with different chemical composition (Banaś et al., 1985; Mikulski and Wierchowiec, 2013; Wierchowiec and Zieliński, 2017; Chapman et al., 2021).

Both imaging modes, SE and BSE, enable the observation of selected parts of grains and the identification of very fine micro-inclusions (<1 μm), the observation of which often exceeds the possibilities of microscopic examination in reflected light (Kania, 2018, 2023; Kania and Muszer, 2024). Determining the mineralogical and chemical composition of micro-inclusions is crucial in this case, as it allows for direct identification of paragenesis and determination of the crystallization environment of gold. Micro-inclusion studies significantly complement the morphological and chemical analyses of gold grains, performed as part of the prospection of primary Au occurrences (Leake et al., 1995; Styles, 1995; Chapman et al., 2023).

GEOLOGICAL SETTING

The study area is located within a segment of the Fore-Sudetic Block which, together with the relatively uplifted Sudetic Block, forms the upper structural unit of the Lower Silesian Block, covering the northeastern part of the Bohemian Massif (Mazur et al., 2006; Żelaźniewicz and Aleksandrowski, 2008; Żelaźniewicz et al., 2011). These two blocks are separated by the Sudetic Marginal Fault (Fig. 1), which extends in a NW–SE direction and was reactivated during the Miocene (Aramowicz et al., 2006; Badura et al., 2007).

The local crystalline basement of this block is likely composed of the deeper Cadomian orogen (Żelaźniewicz, 1997; Żelaźniewicz et al., 1997) and the Luboradz Unit, which forms part of the Kaczawa Metamorphic Complex. The Luboradz Unit consists of a thick succession of sericite-quartz schists (phyllites), greenschists, siliceous schists with quartzites, and greywacke schists, with ages ranging from the Cambrian to the Lower Carboniferous (Baranowski et al., 1990; Kryza and Muszyński, 2003; Urbański and Różański, 2016). This unit constitutes the eastern part of the Saxo-Thuringian Zone, where lithospheric shortening, closure of the sedimentary basin, and the formation of an accretionary prism occurred during the Variscan orogeny (Żelaźniewicz, 2003, and references therein).

In the section where riverbed sediment samples were collected, the Wierzbiak River flows through the southwestern part of the orthogneiss Wądroże Wielkie Massif (Fig. 2). The meta-

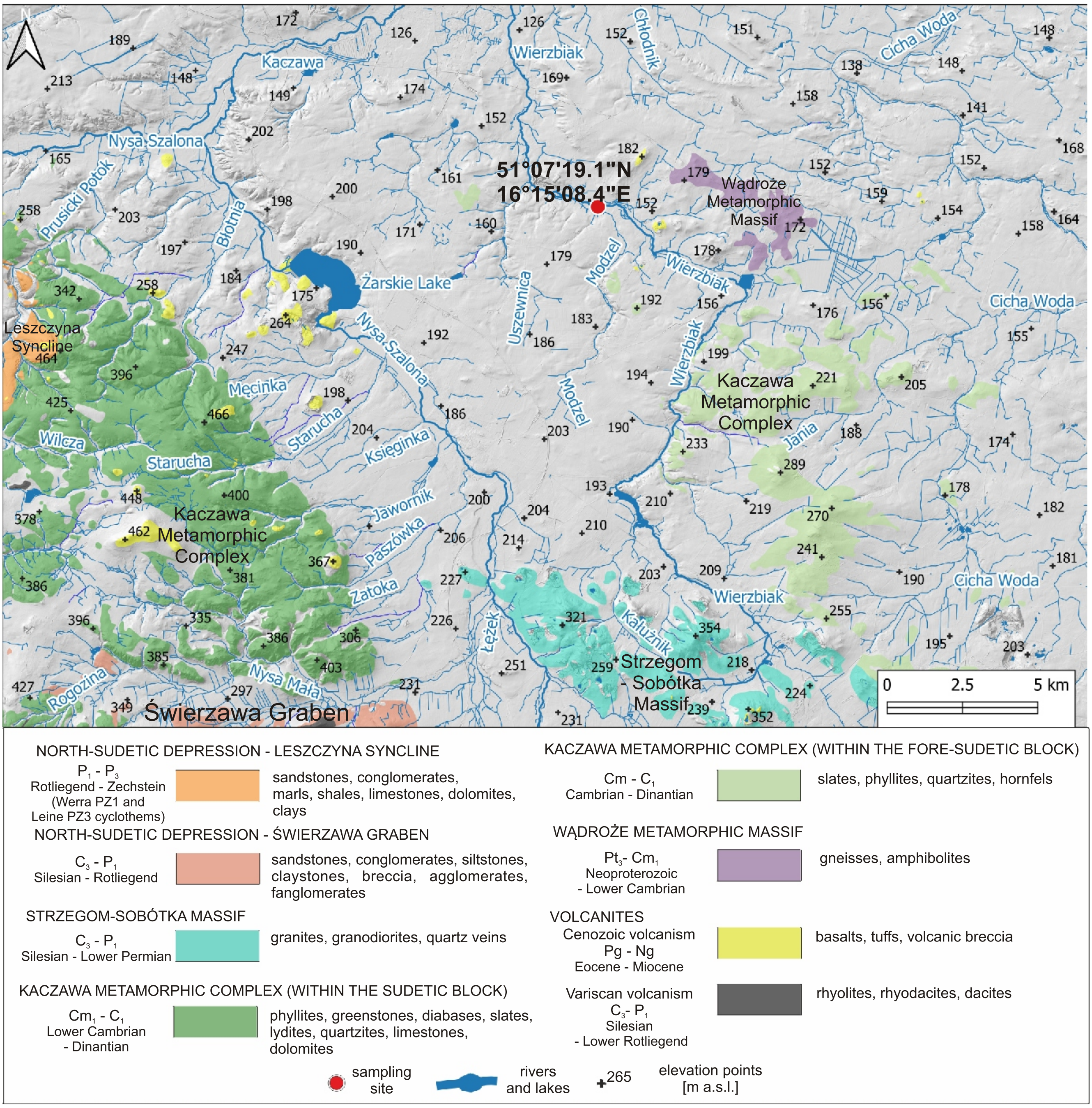

Fig. 2. Compilation of simplified covered geological map and relief map

Compiled after Kozdrój (2009), Przybylski (2009), Urbański (2009a, b), Kozdrój et al. (2012), Cwojdziński and Kozdrój (2013). For location of the area see Figure 1

morphic rocks forming this massif are the oldest in the surrounding area, radiometrically dated to the late Neoproterozoic or early Cambrian (Żelaźniewicz et al., 2004; Żelaźniewicz and Aleksandrowski, 2008). The massif, elongated in a NW–SE direction, is a horst structure, likely uplifted during the Cenozoic, and bordered by the Kaczawa Metamorphic Complex through a local dislocation system. The outcrop of the massif is situated between Mikołajowice, Augustów, and Wądroże Mały, with an additional smaller horst-like structure near Taczalin (Urbański and Różański, 2016).

Within the massif, two types of gneiss have been identified. The first is represented by two-feldspar gneiss, composed of quartz, microcline, albite, biotite and muscovite, with accessory Fe oxides, zircon and garnet. The second is represented by single-feldspar gneiss, transitioning into albite-chlorite schists consisting of quartz, muscovite, and albite, with additional chlorite- and apatite-group members, pyrite, and ilmenite (Kossowska, 1975; Berezowska and Berezowski, 1979).

Alongside the orthogneisses, amphibolites occur, primarily composed of hornblende and plagioclase, with subordinate quartz, apatite, garnet and Fe oxides (Urbański and Różański, 2016).

To the south and southwest of the sampling site, the extensive Strzegom-Sobótka granite Massif, dated to the Late Carboniferous–Early Permian, is present. The Wierzbiak River briefly drains the northwestern part of this granitoid massif, with its source located between Rogoźnica, Graniczna, and Żółkiewka. In this area, Kural and Jerzmański (1974) identified medium- and fine-crystalline biotite granites. According to Domańska-Siuda (2007a, b), local exposures show hornblende-biotite granites, composed of quartz, plagioclase (albite-andesine), alkali feldspar (mainly perthitic microcline), hornblende and biotite, with minor zircon, epidote, allanite, titanite, ilmenite and rutile. This granite variety also contains numerous finely crystalline enclaves of dioritic, granodioritic and tonalitic composition, ranging from several centimetres to several tens of centimetres in size.

Dating of both the granite and the enclaves using the Rb-Sr method yielded an intrusion age of 285.1 ±8.5 Ma to 278 ±7 Ma (Pin et al., 1989; Domańska-Siuda et al., 2004). Near Goczałków, in the immediate vicinity of the granite massif, a contact-metamorphosed cover is present, composed predominantly of sericite-quartz schists, with subordinate spotted schists and hornfels (Urbański and Różański, 2016).

The granite intrusion is intersected by aplite and pegmatite veins. Aplites are distinguished from granite by their finely crystalline structure, white to ash-grey colour, and negligible biotite content (Urbański and Różański, 2016). In the case of pegmatites, the following patterns within the massif have been observed: in the western part, drusen (miarolitic) pegmatites co-occur with vein pegmatites; in the eastern part, vein pegmatites dominate, containing beryl and garnet. This differentiation is attributed to varying depths of crystallization of residual magma in both parts of the Massif (Janeczek, 1985).

Quartz veins cutting through the Wądroże metamorphic feature are of a similar age to the Strzegom-Sobótka granite Massif. According to Majerowicz (1963), they formed during the Sudetes phase of the Variscan orogeny. These quartz veins typically exhibit a NW–SE or N–S orientation, with thicknesses reaching 35 m and lengths of up to 1 km. Their primary constituents, apart from milky quartz, include kaolin and sericite (Czyżowa and Majerowicz, 1965; Berezowska and Berezowski, 1979). Permo-Mesozoic strata are preserved only in the Sudetic Block, filling the North-Sudetic Depression with clastic and carbonate rocks (Fig. 2).

The alluvial deposits of the Wierzbiak River Valley constitute part of the Cenozoic sedimentary cover, deposited directly on the metamorphic-magmatic basement of the Fore-Sudetic Block. In the Paleogene, sedimentation commenced within grabens and tectonic depressions. By the Oligocene, intraplate basaltic volcanism had developed, continuing into the Miocene, when increased tectonic activity led to the uplift of the Sudetic Block relative to the Fore-Sudetic Block. This process resulted in the formation of grabens and horsts, which were subsequently filled with clastic and organic sediments.

During this time, extensive weathered formations developed on Paleozoic crystalline rock outcrops, forming thick clayey regolith covers. A warm, humid climate caused intense chemical weathering, leading to the enrichment of regolith with kaolin, illite and montmorillonite. In local tectonic depressions, where erosion was limited, these regolith covers have been preserved, reaching thicknesses of over 100 metres (Urbański and Różański, 2016).

Basaltic formations near Mikołajowice, Pawłowice Wielkie, and Janowice occur mainly as lava flows, occasionally accompanied by tuffs. These basalts primarily consist of olivine (chrysolite) and pyroxene phenocrysts, embedded in a groundmass composed of calcium monoclinic pyroxenes, olivine, and Ti-Fe oxides (Badura et al., 2005). Additionally, ultramafic rock enclaves have been documented within these volcanic units (Urbański and Różański, 2016, and references therein). K-Ar dating of basalts from Mikołajowice and Pawłowice Wielkie by Birkenmajer et al. (2004) indicates an Oligocene–Lower Miocene age.

Lower and Middle Miocene deposits in the study area are predominantly silts, clays and lignites. The Poznań Formation (Middle Miocene–Pliocene) consists of clay-sand facies deposits with dispersed organic matter and occasional carbonaceous clay interbeds. The Gozdnica Formation, the youngest Neogene unit (Upper Miocene–Pliocene), is composed of coarse-grained alluvial deposits (Urbański and Różański, 2016).

Pleistocene postglacial deposits formed during three glaciations. The Lower Pleistocene and the South Polish Glaciation (Mindel) are represented by fluvioglacial yellow sands and gravels, and dark boulder clays with admixtures of carbonaceous clay and xylites. The deposits of the Middle Polish Glaciation (Riss) include glaciofluvial sands and gravels, glacial silts and tills. The North Polish Glaciation (Würm) is represented by floodplain terrace sands and gravels, and loess and loess-like clays. Holocene deposits include silts filling meltwater depressions, river sands and gravels forming flood terraces, and alluvial soils and peat deposits (Urbański and Różański, 2016).

The GPS coordinates marked on the map define the NW and SE corners of the area shown in Figure 2.

MATERIAL AND METHODS

The sampling site is located in the middle section of the Wierzbiak River, a right-bank tributary of the Kaczawa River, between the villages of Strachowice, Lubień and Ogonowice, ~70–80 m downstream from the mouth of the Modzel tributary. The selection of the sampling site location was an attempt to identify gold grains occurring in the Wierzbiak River channel-fill sediments deposited farther west, beyond the previously documented area of occurrence of detrital alluvial gold (Grodzicki, 1966, 1972; Mikulski and Wierchowiec, 2013). In this section, the river flows through a wide valley and is characterized by a relatively gentle current, which facilitates the accumulation of fine-grained sediments, including muds and clay. The low-energy flow, reflected in the fine-grained nature of the deposited material, resulted in a low concentration of gold in the riverbed sediments. Consequently, only nine gold grains were recovered and prepared for further analysis. However, the primary objective of the fieldwork was to obtain sufficient gold grains to identify micro-inclusions of ore minerals, which had not been studied in earlier publications. In this case, their occurrence was identified in 2 of the grains analysed (including one grain containing as many as 13 distinct micro-inclusions). In previously studied populations of detrital gold, the proportion of grains containing them was not as great (see Kania, 2018, 2023; Kania and Muszer, 2024).

The sampling process was purely qualitative, aiming to obtain a sufficient quantity of material for research rather than determining the concentration of gold grains within the river section studied. To enhance the initial in-situ gravity separation of gold from low-concentration sediments, a modified Henderson hand pump coupled with a Mobile Gravity Concentrator (MGC) was employed (see Kania, 2020; Muszer et al., 2016). The total volume of the input material processed using the MGC during sampling amounted to 0.076 m^3, yielding a pre-concentrate of 266 g under field conditions.The pre-concentrated material was sieved using a 2 mm mesh. After macroscopic identification and manual selection of coarser gold grains, the material was further processed at the Department of Economic Geology, Institute of Geological Sciences, University of Wrocław. The separation was carried out using a Wilfley-type concentrating table with multiple reprocessing cycles. Ultimately, the mass of the final concentrate obtained after gravity separation amounted to 20 g, which corresponds to an estimated mass of 263 g of the heavy mineral fraction per 1 m^3 of sediment. Such trace amounts of gold occurring in the local sediments had already been reported by Mikulski and Wierchowiec (2013), who described its concentration in samples of eluvial, colluvial, and alluvial sediments as "from trace to 0.12 g/m^3".

Polished sections of the gold grains recovered were prepared by embedding them in hardened epoxy resin. Grinding and polishing were performed using Struers metallographic materials, including Piano diamond discs and MD polishers with dedicated polishing pastes.

The qualitative assessment of grain morphology was based on the simplified classification by DiLabio (1991), which distinguishes three categories: *pristine grains*, characterized by their original irregular and angular shapes; *modified grains*, showing signs of abrasion but retaining some original features; and *reshaped grains*, which are rounded due to prolonged transport and abrasion.

To compare grain morphology based on cross-sectional shape observed in reflected light, an original quantitative comparative analysis was employed. This analysis involved calculating the dimensionless K index for each grain analysed. The K index represents the ratio of the grain's cross-sectional perimeter to the circumference of a circle with an equivalent area, thereby accounting for the effective porosity of the grains (see Kania and Muszer, 2024). The rationale for using this parameter lies in the abrasion process of gold grains which, as they migrate in a supergene environment, gradually become more rounded and lose their original irregular shapes (DiLabio, 1991; Townley et al., 2003). As abrasion progresses, the K index decreases, approaching a value of 1 (Kania, 2020). A key advantage of this method is its applicability to the quantitative, statistical comparison of different grain populations.

Contour delineation and length measurements were performed on high-resolution BSE images, which provide strong contrast between the gold grains and their surroundings. The contours were digitized as polygons with vertices spaced at an average distance of 77 nm, and their lengths were measured using *Surfer* software (*Golden Software*).

Chemical composition analysis, as well as the search for and preliminary identification of micro-inclusions, was conducted in reflected light using a *Nikon Eclipse LV100 POL* polarizing universal microscope. For objects smaller than 10 μm, a digital display coupled to the microscope enabled observations at magnifications of up to 2500×. Findings from reflected light microscopy were verified through micro-area analyses using a FEI Quanta scanning electron microscope, equipped with SDD-generation EDS detectors from the XFlash series and *Bruker Esprit v1.9* software. In total, 28 point analyses, 1 linear analysis and 84 elemental maps were made of the micro-inclusions. A detailed description of the SEM-EDS methodology is provided in the Appendix 1. Despite the strictly applied measurement methodology described in the Appendix 1 – including detector calibration, manual interpretation of spectra and precise peak analysis – the results obtained and described of point analyses should be regarded as semi-quantitative, in which the exact elemental composition cannot be determined without the use of standards.

OCCURRENCE OF GOLD ORE MINERALIZATION IN THE STUDY AREA

Both primary and secondary gold occurrences are known in the study area. The primary mineralization, although relatively poor, is associated with Carboniferous quartz veins that cut through the metamorphic rocks of the Wądroże Wielkie Massif. These veins vary in thickness from a few centimetres to up to 35 m, with lengths of up to several hundred metres (Kozłowska-Koch, 1959; Uberna, 1959; Czyżowa and Majerowicz, 1965; Berezowska and Berezowski, 1979; Żelaźniewicz and Aleksandrowski, 2008; Mikulski and Wierchowiec, 2013). Within these veins, microscopic gold (<0.2 mm) occurs alongside submicroscopic gold, which is concentrated in pyrite with an average content of 1.6 ppm (Zöller and Heuseler, 1926; Grodzicki, 1966).

Secondary gold occurs in various sedimentary environments, comprising local kaolinized regolith formed *in situ* on the outcrops of the Wądroże Massif, and colluvial and alluvial sediments of the Wierzbiak River. Mikulski and Wierchowiec (2013) conducted comparative studies on the morphology and chemical composition of gold grains collected from these types of deposit. Their studies revealed marked differences in gold content, grain size, morphology and concentration across the sedimentary types.

In the alluvial sediments, larger grains (up to 1.5 mm) are generally more flattened and rounded, commonly with bent edges and a lack of inclusions or overgrowths. These grains commonly show Ag-depleted rims and, in some cases, a porous structure.

In contrast, eluvial gold retains relic features of its primary morphology, with narrower Ag-depleted rims and a small proportion (1–2%) of porous grains. Mikulski and Wierchowiec (2013) also observed morphological changes in gold grains along the river course, noting a progressive downstream increase in grain rounding, consistency of shape, and the proportion of flake-shaped grains.

Gold from the colluvial deposits shows intermediate features, including visible abrasion marks and frequent mineral inclusions, e.g., rutile and clay minerals (Wierchowiec, 2010; Mikulski and Wierchowiec, 2013).

RESULTS

MORPHOLOGY AND CHEMICAL COMPOSITION

A detailed analysis of chemical and mineralogical composition was conducted on nine detrital gold grains collected from the Wierzbiak River bed sediments. Eight grains show rounded edges and oval shapes, characteristic of the *reshaped* morphological class. One grain (W-1) displays features of the *modified* class, with partially rounded and blunted sharp edges, suggesting limited mechanical abrasion while retaining an overall irregular morphology. This is reflected in the K index values, which are generally < 2.0, except for two grains: W-2 and W-4 (Fig. 3). These two grains display rounded edges and a distinct spongy internal texture, developed throughout the entire grain volume, aligning morphologically with amalgamate-type grains of an-

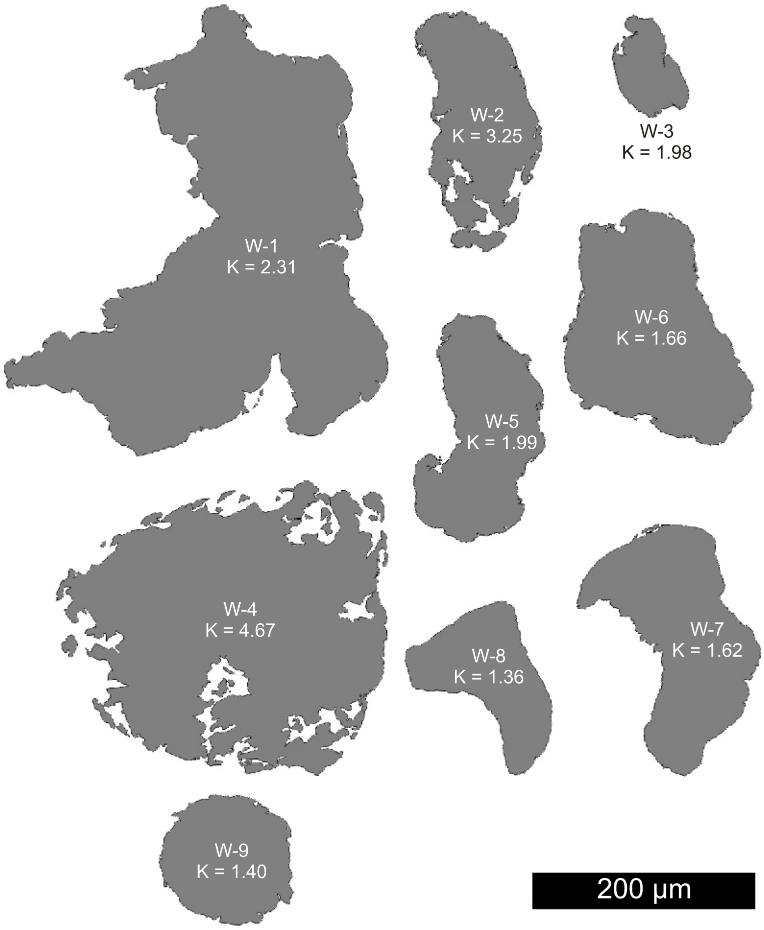

Fig. 3. Outlines of the gold grains analyzed in detail, shown in relation to their calculated K index values

thropogenic origin previously documented in Holocene sediments of the Skora River (Muszer et al., 2016; Kania and Muszer, 2024). The grains vary in circumference from 95 µm to 455 µm, with an average diameter of 260 µm.

The chemical composition of the grain population is relatively homogeneous, with silver identified as the only significant impurity, approaching 20 wt.%. Notably, grains W-1 and W-3 exhibit zones of elevated silver content, located both internally and along their edges (Fig. 4), whereas in the remaining grains, silver is more uniformly distributed across the sections analysed (Figs. 5 and 6). No grains with distinct Ag-depleted rims were identified in the sample studied.

Grains W-1, W-3, W-5 and W-7 revealed intra-grain variations in Ag content (Fig. 4), suggesting internal heterogeneity, while the other grains show a more uniform composition. Based on the phase composition, all grains are composed of native gold (*sensu* Yushko-Zakharova et al., 1986). The results of the analyses of Ag content in individual grains are shown in tabular form in Appendix 1.

The presence of mercury was not conclusively confirmed, including in porous W-2 and W-4 grains. Neither series of point analyses nor detailed analyses of the spectra obtained revealed Hg concentrations exceeding the detection limit of 0.1 wt.%, adopted as a detection limit for the analytical method used.

MICROINCLUSIONS

No inclusions of rock-forming minerals were identified in the gold grain population studied. Despite the small population of sampled grains, a notably rich population of 13 microinclusions of ore minerals was documented.

These inclusions vary in size from submicrometre dimensions to ~10 µm. The majority were identified within the reshaped grain W-6 (Fig. 6), which contains the largest and most complex inclusion: a polymineralic, oval aggregate composed of a xenomorphic chalcopyrite crystal intergrown with Ni-Co-Fe sulpharsenides (up to 6 µm across) and a 2-µm galena crystal (Fig. 7). The remaining individual inclusions consist of discrete microinclusions not exceeding 5 µm in size. These are represented by three arsenopyrites (3–5 µm), two pyrites (1 and 2.5 µm), and two Ni-Fe-Co sulpharsenides with diameters <1 µm, most of which have a composition dominated by nickel, resembling gersdorffite. One of the arsenopyrite inclusions displays a distinctly automorphic, rhombohedral habit (Figs. 8 and 9).

In addition, a single oval exsolution inclusion of native bismuth, ~4 µm in diameter and containing trace amounts of tellurium and arsenic, was identified within *reshaped* grain W-9 (Figs. 10 and 11).

DISCUSSION

Despite the limited size of the grain population studied, it is characterized by relatively limited variability in both shape and chemical composition when compared to previously analysed populations from the bed sediments of the Jamna Creek (Kania, 2018), the Skora River and Żeliszowski Creek (Kania, 2023; Kania and Muszer, 2024). The distinct predominance of rounded grains with low K index values suggests their significant transport distance from the source area.

The sampling site is located ~0.5 km downstream from the lowermost alluvial sediment sample collected by Mikulski and Wierchowiec (2013) and the observed differences in the mor-

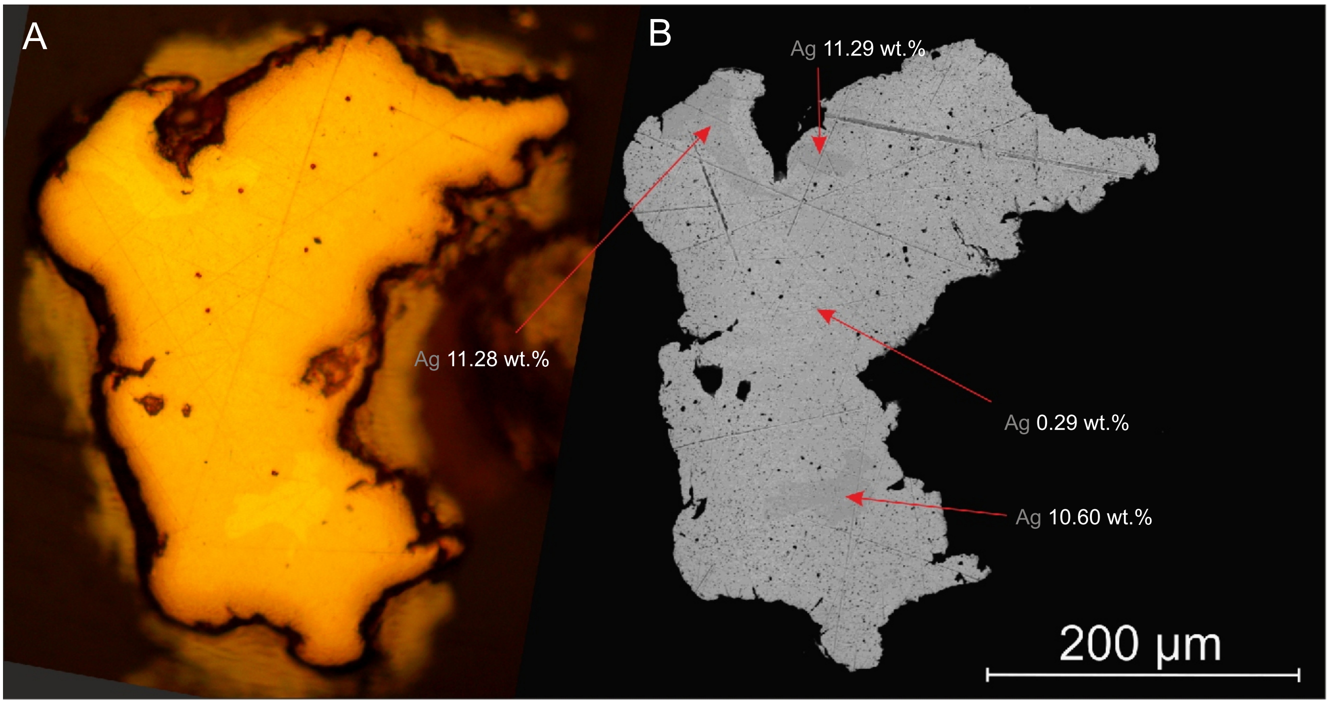

Fig. 4. W-1 gold grain

A – image in reflected light, **B** – BSE image

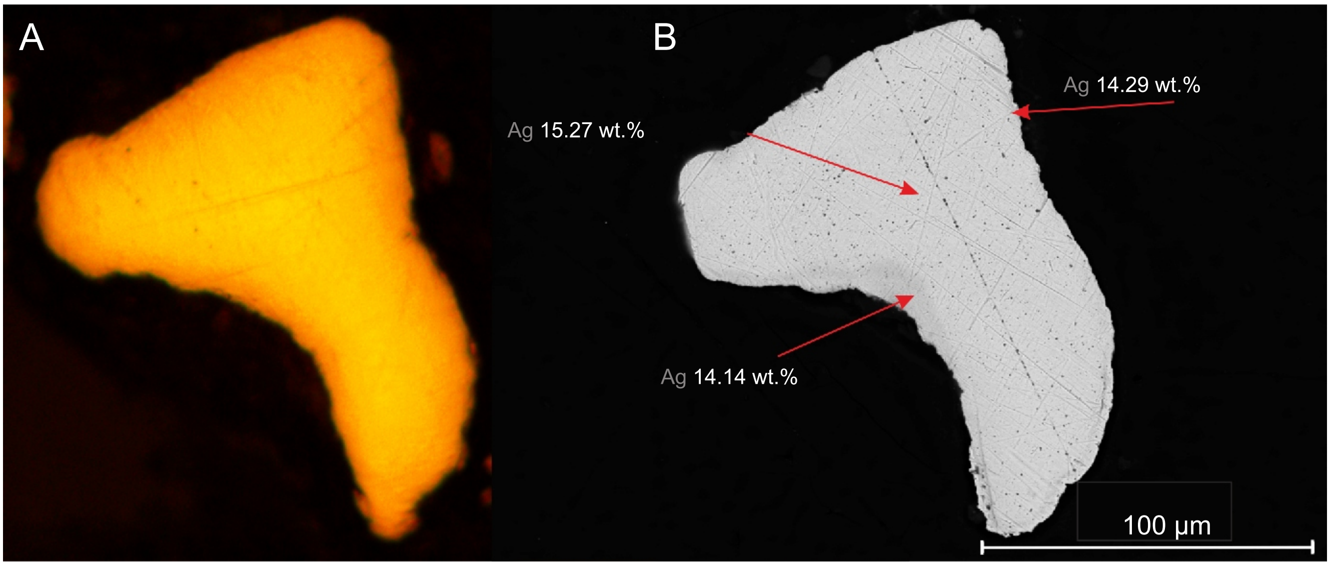

Fig. 5. W-8 gold grain

A – image in reflected light, **B** – BSE image

phology and chemical composition of the gold grains described in their study compared to those analysed herein are significant – none of the grains in the present study show Ag-depleted rims or electrum compositions, nor possess an angular, clearly *pristine* shape. However, the presence of rounded grains with porous structures was confirmed, which were considered by previous authors as products of weathering processes or redeposition from older Cenozoic deposits. Point analyses conducted in this study do not contradict this interpretation: trace Hg concentrations and the absence of discernible and identifiable Hg peaks in the EDS spectra do not provide sufficient evidence to classify the grains analysed as anthropogenic amalgams.

Importantly, the most significant new insights into the genesis and evolution of local placer gold deposits derive not from the grain morphology or bulk chemical composition, but from the mineralogical and chemical characterization of micro-inclusions described in this study.

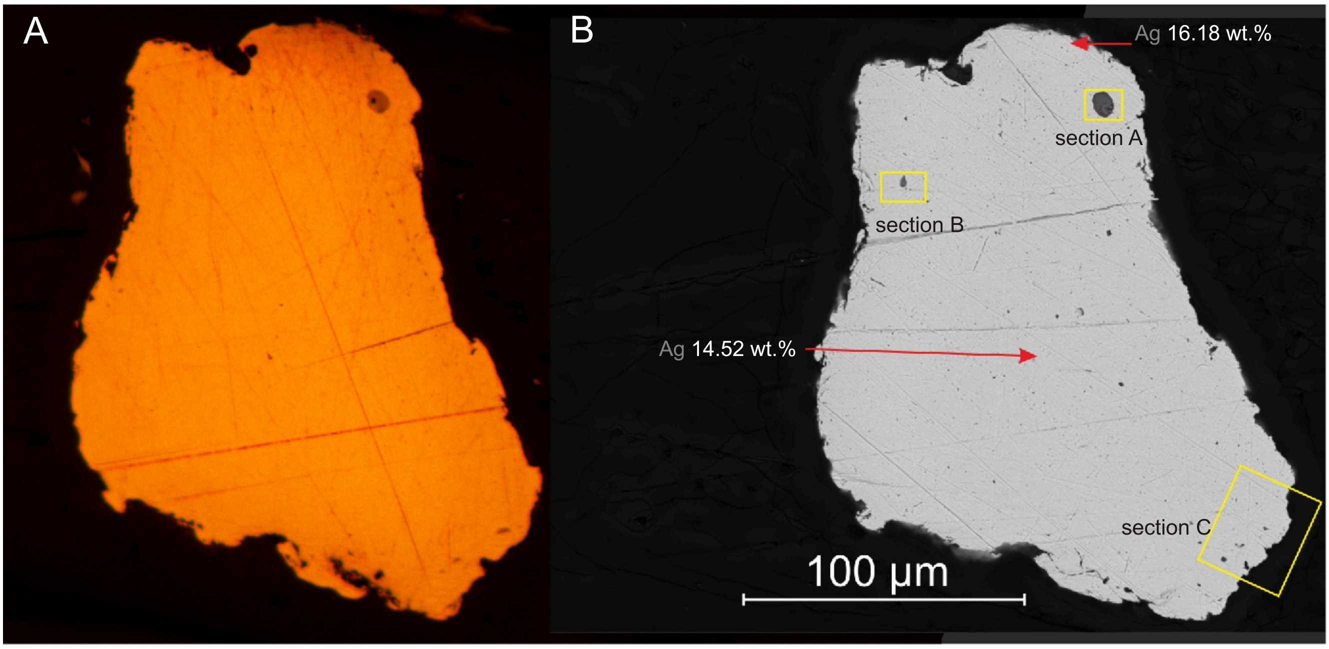

Fig. 6. The ore-bearing W-6 gold grain

A – image in reflected light, **B** – BSE image; location of the sections shown in Figures 7, 8 and 9 marked

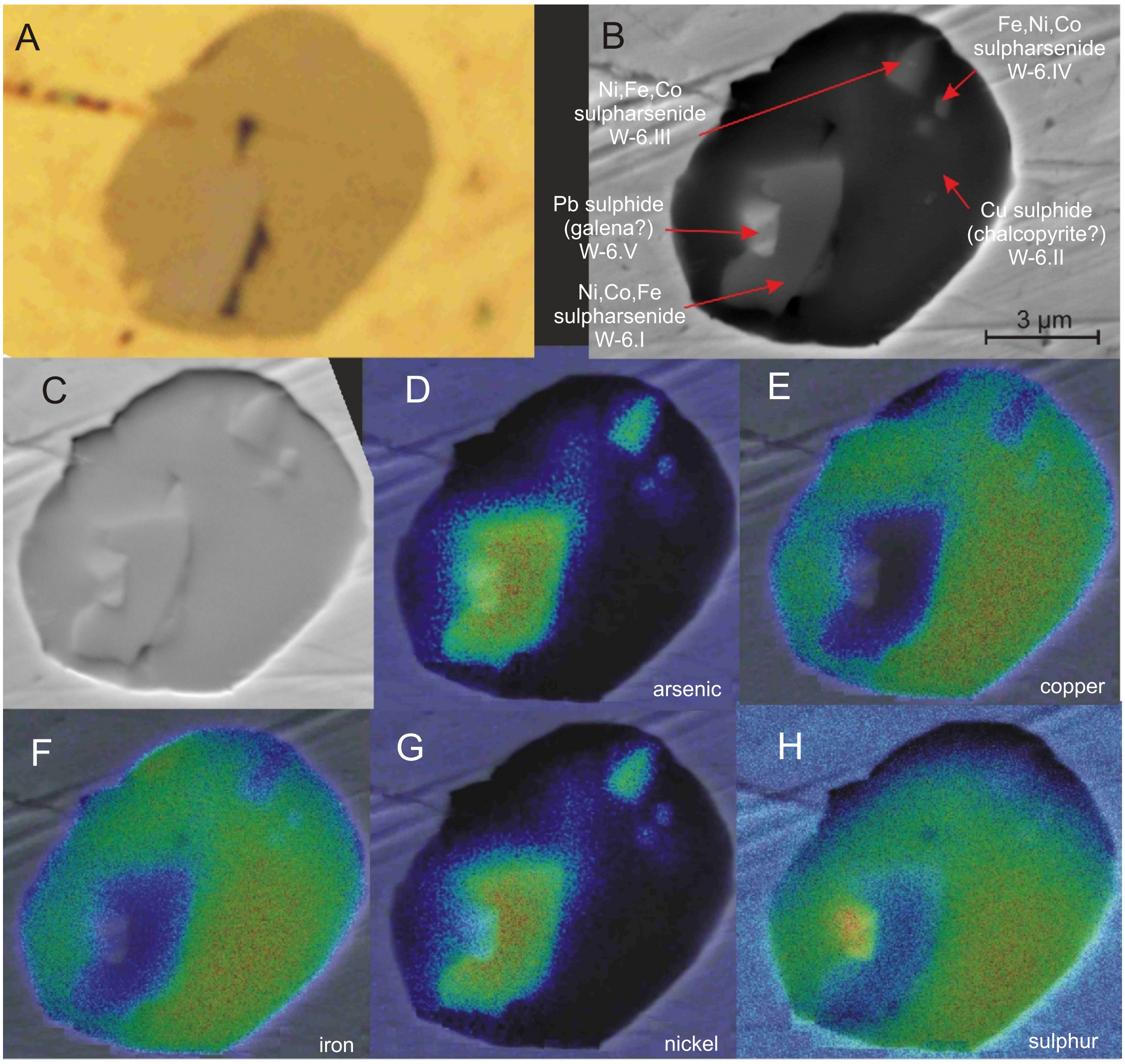

Fig. 7. Enlargement of section A of Figure 6B – polymineralic inclusion of sulpharsenides and sulphides within the W-6 gold grain

A – image in reflected light; **B** – BSE image with location of the point analyses marked (results in Appendix 1); **C** – SE image; **D–H** – distribution of selected elements: black, violet, blue, green up to red colours indicate increasingly high concentrations

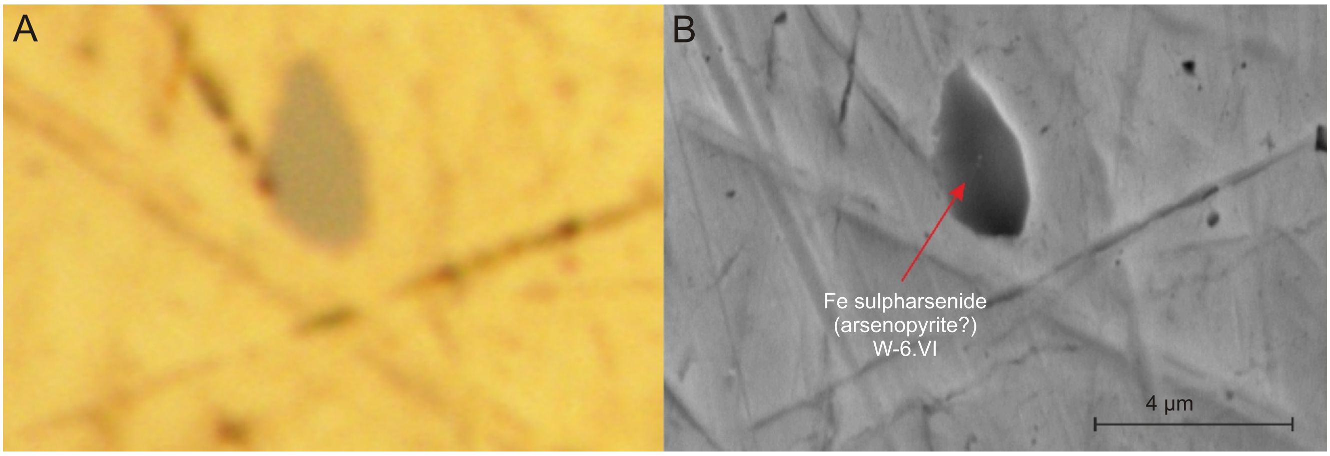

Fig. 8. Enlargement of section B of Figure 6B – inclusion of arsenopyrite composition within the W-6 gold grain

A – image in reflected light; **B** – BSE image with location of the point analysis marked (results in Appendix 1)

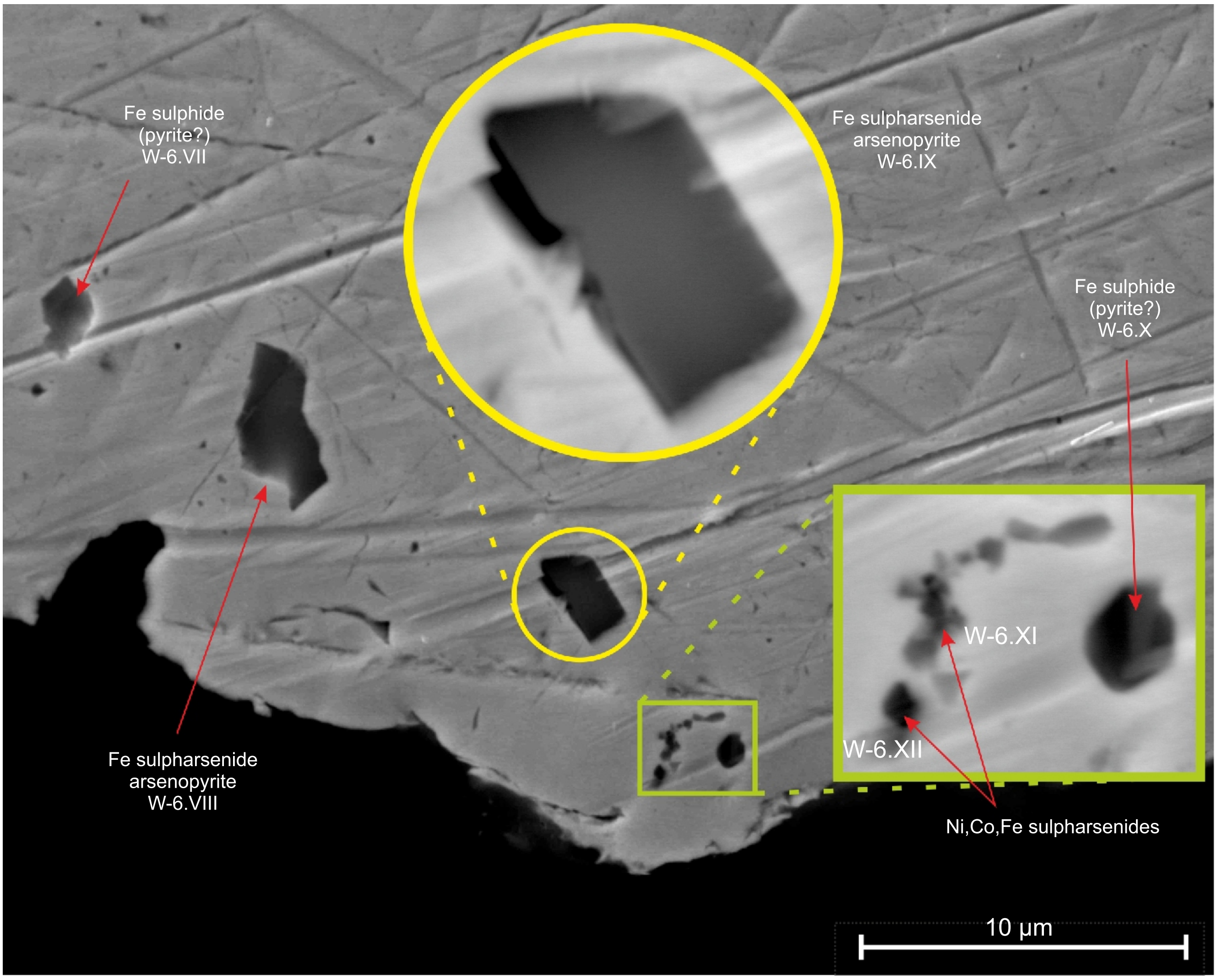

Fig. 9. Enlargement of section C of Figure 6B – inclusions of Fe-Ni-Co sulpharsenides and sulphides within the W-6 gold grain

BSE image with location of the point analyses marked (results in Appendix 1)

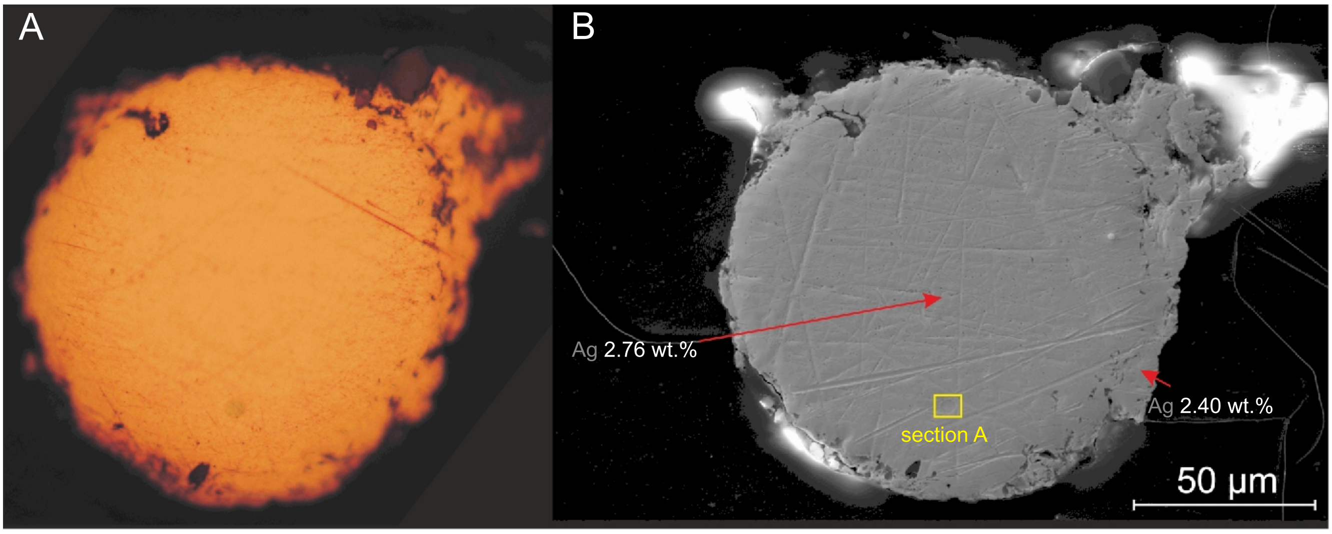

Fig. 10. The ore-bearing W-9 gold grain

A – image in reflected light; **B** – SE image, location of the section shown in Figure 11 marked

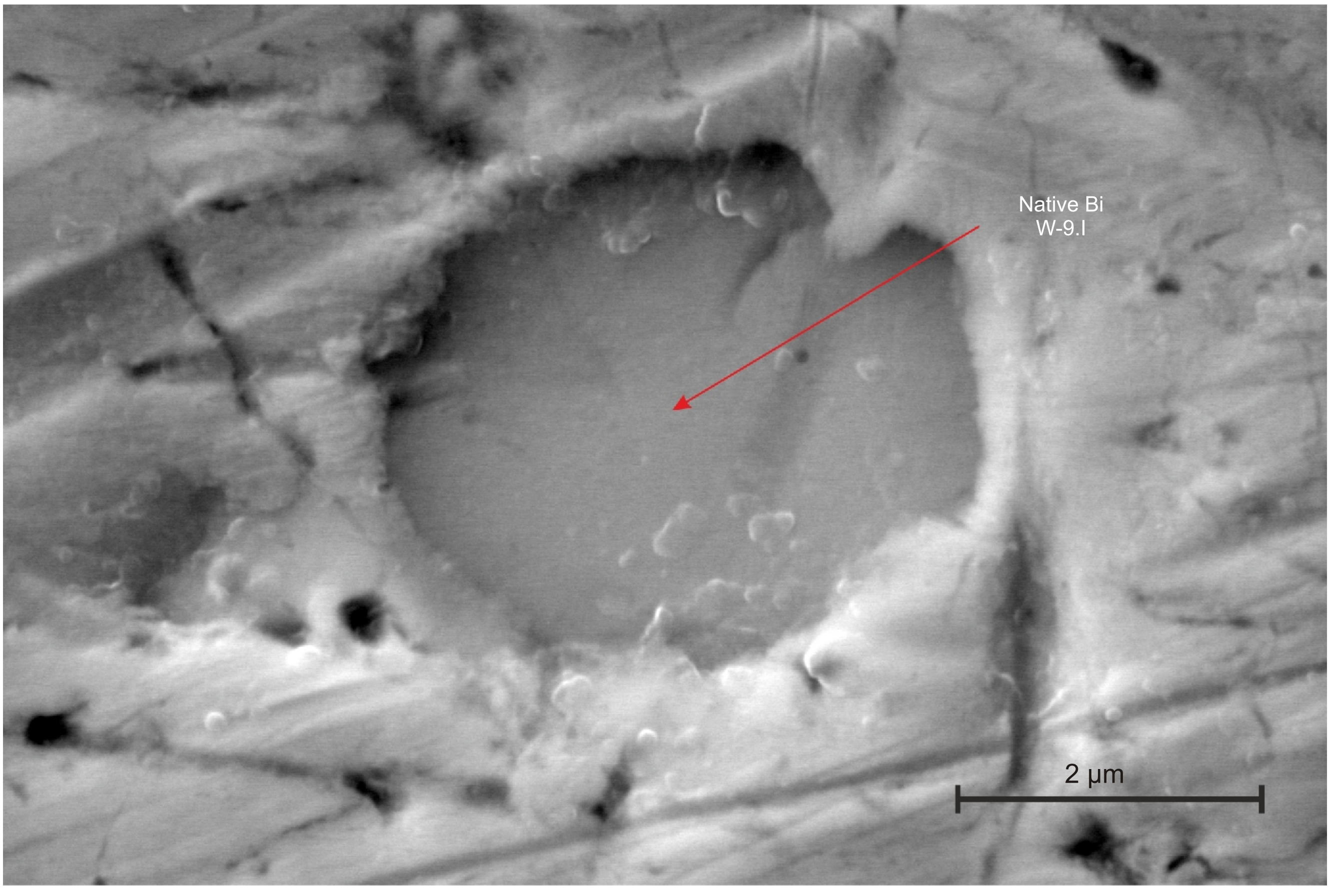

Fig. 11. Enlargement of section A of Figure 10 – phase of native bismuth within the W-9 gold grain SE image with location of the point analysis marked (results in Appendix 1)

It is commonly considered that the primary source of the alluvial gold deposits in the Wierzbiak Valley is the nearby quartz veins that cut through the Wądroże metamorphic Massif. This interpretation is strongly supported by the presence of gold-bearing clasts of vein quartz identified within the weathered eluvial covers developed on the Wądroże gneiss Massif, as well as within the surrounding colluvial deposits. Further support comes from the results of comprehensive comparative analyses of the morphological characteristics of eluvial, colluvial and alluvial gold grains, including studies of grain outlines, shapes, surface structures, mineral intergrowths and overgrowths, and the presence of Ag-depleted rims (Grodzicki, 1972, 1998, and references therein; Banaś et al., 1985; Mikulski and Wierchowiec, 2013).

However, the results of SEM-EDS analyses of micro-inclusions found in two gold grains from the Wierzbiak River bed sediments point to a more complex genesis of the gold-bearing deposits in the Legnickie Pole – Mikołajowice – Wądroże region. Particularly significant is the notable abundance of arsenic, which appears to have been a key component of the crystallization environment in which the identified micro-inclusions formed. Arsenic is present not only in the Ni-Co-Fe sulpharsenides but also in native bismuth and pyrite, in concentrations reaching several weight percent.

By comparison, the quartz gold-bearing veins of the Wądroże gneiss Massif show a qualitatively distinct mineralogical composition (Table 1). Arsenic mineralization in these veins is represented exclusively by a Cu-As sulphosalt (tennantite-group member?). Additionally, mineral phases indicative of higher crystallization temperatures, including pneumatolytic minerals such as cassiterite, titanite, xenotime- and monazite-group members, are also present (Wołkowicz, 2015). According to Wołkowicz (2015), the occurrence of magnetite, chromite, titanite, xenomorphic pyrite and possibly rutile within the quartz veins reflects relics of rock transformation associated with quartz mineralization processes. The high-temperature hydrothermal crystallization of allanite, monazite, xenotime and probably cassiterite is attributed to a postmagmatic origin. By contrast, the presence of automorphic pyrite, sulphosalts, galena, sphalerite, chalcopyrite and probably native bismuth is linked to the activity of low-temperature hydrothermal fluids.

Meanwhile, the micro-inclusions identified within the detrital gold grains analysed are predominantly represented by Ni-Co-Fe sulpharsenides, along with individual sulphides such as pyrite, galena and chalcopyrite, as well as native bismuth. This mineral assemblage closely resembles an ore mineralization found in hydrothermal As-polymetallic veins of the Kaczawa Metamorphic Complex. A similar association of micro-inclusions, represented by galena and numerous Co-Fe-Ni sulpharsenides (with Co-Ni-Fe arsenides?), was previously identified within a detrital gold grain from the Holocene alluvial sediments of the Jamna Creek, which flows through the Wleń Trough near the quartz–polymetallic vein system of the Klecza – Radomice region (Kania, 2018; see Table 1). In these local hydrothermal deposits, the native gold mineralization was preceded by a mesothermal mineral association composed of sulphides, sulpharsenides, and sulphosalts, including pyrite, chalcopyrite, galena, sphalerite, tetrahedrite and cobaltite, as well as electrum (Mikulski, 2007).

In its upper course, the Wierzbiak River also drains the northwestern part of the Strzegom – Sobótka granitoid massif, where a deep erosive cut locally reaches pegmatite mineralization zones. The ore mineral assemblages of pegmatites located in the western part of the massif, outlined in Table 1, represent a typical pneumatolytic and high-temperature range of hydrothermal processes. Notably, these assemblages are devoid of arsenic-bearing phases.

The closest hydrothermal occurrence with significant arsenic mineralization to the sampling site is constituted by the polymetallic veins of the Chełmiec Unit of the Kaczawa Metamorphic Complex, ~15 km to the WSW. These veins exhibit considerable variability in mineral composition (Table 1), with thicknesses ranging from 0.3 to 8 m and lengths from 0.3 to 1 km. While the average gold concentration typically does not exceed 100 ppb, concentrations in two veins – Dębowa near Męcinka and Olejna near Chełmiec – reach 0.344 and 1.01 ppm, respectively (Mikulski, 2007, 2011). Gold in these veins occurs exclusively in submicroscopic form, primarily as an admixture within Ni-Co-Fe sulpharsenides (gersdorffite, cobaltite, arsenopyrite), with a strong positive correlation to the content of As, Ni and Co (Mikulski, 2007). Given this, the clastic material derived from the eroded local quartz veins could not have been the source of the ore-bearing detrital gold in the Wierzbiak sediments.

The Sudetic Block, together with the Fore-Sudetic Block, is tectonostratigraphically homogeneous. However, the surface exposes different intersection levels, which are related to the activity of the Sudetic Boundary Fault and the final, relative uplift of the Sudetic Block (Żelaźniewicz and Aleksandrowski, 2008). The occurrence of As-polymetallic gold-bearing quartz veins is not necessarily confined to the Chełmiec Unit but may extend northeastwards into the Fore-Sudetic Block, where beyond the Strzegom-Sobótka Massif, the veins are buried beneath a cover of Cenozoic strata. This hypothesis aligns with the interpretation proposed by Mikulski and Wierchowiec (2013), who suggested that by the end of the Pleistocene, erosional processes of the local river network reached the basement rocks, additionally eroding older regolith covers and deposits from earlier glaciations. In a broader context, the potential genetic development and relationship between the polymetallic mineralization of the Chełmiec Unit in the Kaczawa Metamorphic Complex, the Fore-Sudetic Block in the area of the Wądroże Wielkie Massif, and the tectonic-magmatic activity of the Strzegom-Sobótka Massif was discussed in more detail by Mikulski (2007: 93–96).

There is also the possibility of deposition of gold-enriched moraines, including material eroded from the Fennoscandian Shield, in the Wierzbiak drainage basin during the Pleistocene glacial advances; Kozłowski (2011) documented the presence of Scandinavian detrital gold in Poland. However, due to the widespread occurrence of gold-enriched polymetallic veins of Fe-Ni-Co-Bi-As type within the Kaczawa Metamorphic Complex, this option should be considered unlikely.

The results described in this paper do not contradict the prevailing view that the great majority of local detrital gold in these alluvial sediments originates from the weathering of quartz veins of the Wądroże Wielkie Unit. In fact, they justify the need for further, more detailed investigations aimed at determining the distribution of detrital gold associated with the Fe-Ni-Co-Bi-As mineralization assemblage in local Cenozoic deposits. These studies should initially focus on systematic sampling of the riverbed sediments of the Wierzbiak River and its tributary, the Modzel River. Interpretations of grain transport directions should consider not only the present-day terrain morphology, but also the local palaeotopography and the occurrence of older Cenozoic deposits, particularly those of Pleistocene age. The preliminary research described in this article, together with the proposed framework for more detailed studies, provide a ratio-

Table 1

Comparison of the qualitative composition of ore minerals (excluding native gold) described from hydrothermal veins of the Wądroże Massif and the Kaczawa Metamorphic Complex

	Ore minerals from quartz veins of the Wądroże metamorphic Massif (Wołkowicz, 2015)	Ore minerals from polymetallic veins of the Chełmiec Unit (Kaczawa Metamorphic Complex) (Paulo, 1970; Mikulski, 2007)	Ore minerals from pegmatites of the W part of the Strzegom – Sobótka Massif (Janeczek, 1985; Ciesielczuk et al., 2008)	Ore mineral micro-inclusions within gold grain from river bed sediments of the Jamna Creek (Wleń Graben) (Kania, 2018)
allanite-group	+			
arsenopyrite		**+**		**?**
azurite		+		
native Bi	**?**	**+**	**+**	
bismuthinite		+	+	
bornite		+		
bournonite		+		
carrolite		+		
cassiterite	+		+	
cerussite		+		
chalcocite	+	+	+	
chalcopyrite	**+**	**+**	**+**	
chromite	+			
cosalite			+	
covellite	+	+	+	
cryptomelane			+	
enargite			+	
fergusonite-(Y) / formanite-(Y) / tantalaeschynite-(Y)			+	
galena	**+**	**+**	**+**	**+**
gersdorffite / nickeline		**+**		**+**
goethite	+	+	+	+
hematite		+	+	
malachite		+		
magnetite	+	+	+	
molybdenite			+	
monazite-group	+		+	
pyrrhotite		?	+	
pyrite / marcasite	+	+	+	
retgersite		+		
rutile	?			
siderite		+		
scheelite			+	
skutterudite		+		
sphalerite	+	+	+	
Cu-As sulphosalt	+			
Cu-Sb sulphosalt	+			
tetrahedrite-group		+		
titanite	+			
uraninite			+	
valleriite			+	
wolframite			+	
wulfenite			+	
xenotime-group	+		+	

+ – presence confirmed, ? – probable presence, ore minerals with a composition similar to the composition of micro-inclusions identified in gold grains W-6 and W-9 are marked in bold nale for improved geophysical exploration of the basement of the Kaczawa Metamorphic Complex in the study area. Such investigations have already been carried out by the Polish Geological Institute using the Very Low Frequency (VLF) electromagnetic method in the Klecza–Radomice region (Mikulski and Ostrowski, 2023), and they align with a broader intent to explore for and identify Au-polymetallic ore deposits within the Fore-Sudetic Block (Szamałek et al., 2020).

CONCLUSIONS

1. The population studied of detrital gold from contemporary Wierzbiak riverbed sediments exhibits low variability in grain shape and a high degree of edge rounding, as indicated by low K index values. This likely reflects a slow rate of grain migration. Similarly, the grains show a relatively homogeneous Au-Ag alloy composition, classified within the native gold phase (*sensu* Yushko-Zakharova et al., 1986) with silver content reaching up to 20 wt.% Ag. However, the differences in the average Ag weight contents between individual grains reach several percentage points. These features distinguish the grains analysed from those collected from sediments of the Wleń and Kaczawskie Foothills areas, where local gold grain populations are characterized by greater morphological and chemical diversity, including grains composed of native gold, metastable and electrum phases (see Kania, 2018, 2023; Kania and Muszer, 2024).

2. Despite the paucity of grains obtained for analysis, detrital gold was found in the alluvial sediments of Wierzbiak up to the mouth of the Modzel River tributary. These results should be considered preliminary, justifying further exploration for Au-polymetallic mineralization in the Wierzbiak River basin area, and in particular along the Modzel tributary.

3. The microinclusions observed in the gold grains analysed represent a typical Fe-Ni-Co-Bi-As hydrothermal mineralization assemblage, dominated by Ni-Co-Fe sulpharsenides and As-bearing sulphides, including pyrite, chalcopyrite, galena and native bismuth. This paragenesis of the micro-inclusions does not correspond to the mineralogical assemblages identified in the quartz veins of the Wądroże Wielkie Massif, nor to the pegmatite-hydrothermal mineralization of the Strzegom-Sobótka Massif. Instead, it is consistent with the ore mineralization characteristic of the polymetallic quartz veins in the Chełmiec Unit, part of the Kaczawa Metamorphic Complex. However, the presence of gold in these veins was confirmed exclusively in submicroscopic form, as a trace admixture in sulpharsenides.

4. The results of this study support a hypothesis of complex genesis for the local gold-bearing placer deposits. While most gold grains occurring in the Wierzbiak River sediments likely originate from the weathered quartz veins intersecting the Wądroże Wielkie Massif, the micro-inclusions identified suggest the possible contribution of gold sourced from the other primary gold-bearing deposits within the Kaczawa Metamorphic Complex: eroded over time, their gold-bearing material may have been subsequently included in the Cenozoic deposits of the Fore-Sudetic Block.

5. Previous studies of micro-inclusions in detrital gold from the Cenozoic deposits of Lower Silesia indicate a dual origin for the gold-bearing material. Gold grains in the local placer deposits were sourced from the weathering of two types of primary deposit: (1) the Carboniferous quartz-polymetallic veins of the Kaczawa Metamorphic Complex and the Wądroże Wielkie Massif, and (2) the Permian ore-bearing deposits of red beds-type, filling the North Sudetic Depression. The gold-bearing deposits of the Kaczawa-Izera Foothills formed as a result of weathering and accumulation of rock material from both deposit types (Kania, 2018, 2023; Kania and Muszer, 2024), while the Wądroże region's placer deposits originate from the first type. Furthermore, the potential incorporation of the detrital gold from weathering pegmatite formations, Pleistocene glacial deposits and Au-bearing rocks of the Fennoscandian Shield into the Lower Silesian Cenozoic placer deposits remains a subject for further exploration (see Jęczmyk and Krzemińska, 1996; Grodzicki, 2011; Kozłowski, 2011; Kania, 2023).

Acknowledgements. The author would like to thank the editors and reviewers for their constructive comments, which significantly improved the manuscript. Special thanks go to Dr. A. Muszer for expert advice, particularly regarding mineralogical analyses in reflected light.

Funding. Article prepared within the framework of the PGI-NRI publication project (No. 62.9012.2518.00.0), financed by subsidy from the Ministry of Science and Higher Education.

REFERENCES

Aramowicz, A., Anczkiewicz, A.A., Mazur, S., 2006. Fission-track dating of apatite from the Góry Sowie Massif, Polish Sudetes, NE Bohemian Massif: implications or post-Variscan denudation and uplift. Neues Jahrbuch für Mineralogie Abhandlungen, **182**: 221–229; https://doi.org/10.1127/0077-7757/2006/0046

Badura, J., Pécskay, Z., Koszowska, E., Wolska, A., Zuchiewicz, W., Przybylski, B., 2005. New data on age and petrological properties of Lower Silesian Cenozoic basaltoids, SW Poland (in Polish with English summary). Przegląd Geologiczny, **54**: 145–153.

Badura, J., Zuchiewicz, W., Štěpančiková, P., Przybylski, B., Kontny, B., Cacoń, S., 2007. The Sudetic Marginal Fault: A young morphotectonic feature at the NE margin of the Bohemian Massif, Central Europe. Acta Geodynamica et Geomaterialia, **4** (148): 7–29.

Banaś, J., Grodzicki, A., Salamon, W., 1985. Mineralogic-geochemical characterization of detrital native gold from the vicinity of Złotoryja and Wądroże Wielkie, Lower Silesia, SW Poland. Mineralogia Polonica, **16**: 91–114.

Baranowski, Z., Haydukiewicz, A., Kryza, R., Lorenc, S., Muszyński, A., Solecki, A., Urbanek, Z., 1990. Outline of the geology of the Góry Kaczawskie (Sudetes, Poland). Neues Jahrbuch für Geologie und Paläontologie Abhandlungen, **179**: 223–257.

Berezowska, B., Berezowski, Z., 1979. Objaśnienia do Szczegółowej Mapy Geologicznej Sudetów 1:25 000, arkusz Wądroże Wielkie (in Polish). Wydaw. Geol., Warszawa.

Birkenmajer, K., Pécskay, Z., Grabowski, J., Lorenc, M.W., Zagożdżon, P.P., 2004. Radiometric dating of the Tertiary volcanics in Lower Silesia, Poland. IV. Further K-Ar and palaeomagnetic data from Late Oligocene to Early Miocene basaltic rocks of the Fore-Sudetic Block. Annales Societatis Geologorum Poloniae, **74**: 1–19.

Chapman, R., Leake, B., Styles, M., 2002. Microchemical characterization of alluvial gold grains as an exploration tool. Gold Bulletin, **35**: 53–65; https://doi.org/10.1007/BF03214838

Chapman, R.J., Banks, D.A., Styles, M.T., Walshaw, R.D., Piazolo, S., Morgan, D.J., Grimshaw, M.R., Spence-Jones, C.P., Matthews, T.J., Borovinskaya, O., 2021. Chemical and physical heterogeneity within native gold: implications for the design of gold particle studies. Mineralium Deposita, **56**: 1563–1588; https://doi.org/10.1007/s00126-020-01036-x

Chapman, R., Mortensen, J. K., Murphy, R., 2023. Compositional signatures of gold from different deposit types in British Columbia, Canada. Minerals, **13**, 1072; https://doi.org/10.3390/min13081072

Ciesielczuk, J., Domańska-Siuda, J., Szuszkiewicz, A., Turniak, K., 2008. Strzegom-Sobótka massif (Sudetes, SW Poland) – an example of a complex Late-Variscan granitic intrusion and its pegmatitic mineralization. Conference: Mineralogia – Special Papers, **32**: 181–188; https://doi.org/10.13140/RG.2.1.4473.4564

Cwojdziński, S., Kozdrój, W., 2013. Szczegółowa Mapa Geologiczna Polski, 1:50 000, arkusz 796 – Wojcieszów (in Polish). Państw. Inst. Geol. – PIB, Warszawa.

Czyżowa, T., Majerowicz, A., 1965. Preliminary data on quartz deposit at Taczalin near Legnica (in Polish with English summary). Przegląd Geologiczny, **13**: 151–155.

Dadlez, R., Marek, S., Pokorski, J., Buła, Z., 2000. Mapa geologiczna Polski bez utworów kenozoiku 1:1 000 000 (in Polish). Wydaw. Kartograficzne PAE, Warszawa.

DiLabio, R.N.W., 1991. Classification and interpretation of the shapes and surface textures of gold grains from till. Gisements alluviaux d'or, La Paz, 1–5.06: 297–313.

Domańska-Siuda, J., 2007a. Pochodzenie i ewolucja stopu macierzystego granitu hornblendowo-biotytowego z zachodniej części masywu strzegomskiego (in Polish). Przegląd Geologiczny, **55**: 284.

Domańska-Siuda, J., 2007b. The granitoid Variscan Strzegom-Sobótka massif. Archivum Mineralogiae Monograph, **1**: 179–191.

Domańska-Siuda, J., Bachliński, R., Słaby, E., 2004. Studium izotopowe Rb-Sr i Sm-Nd granitu hornblendowo-biotytowego z masywu Strzegom-Sobótka i jego enklaw (in Polish). 7 Ogólnopolska Sesja Naukowa Datowanie Minerałów i Skał: 14–18.

Domaszewska, T., 1964. Occurence and exploitation of gold in Lower Silesia (in Polish with English summary). Przegląd Geologiczny, **12**: 180–184.

Dziekoński, T., 1972. Wydobywanie i metalurgia kruszców na Dolnym Śląsku od XIII do połowy XX wieku (in Polish). Wydaw. PAN, Zakład Narodowy im. Ossolińskich, Wrocław: 103–132.

GeoLOG. Application of the Central Geological Database (CBDG) of Polish Geological Institute – National Research Institute; https://geolog.pgi.gov.pl

Grodzicki, A., 1966. Auriferous sands from Legnickie Pole – Mikołajowice – Wądroże Wielkie (in Polish with English summary). Archiwum Mineralogiczne, **26**: 1–2.

Grodzicki, A., 1972. On the petrography and mineralogy of the gold-bearing sands of Lower Silesia (in Polish with English summary). Geologia Sudetica, **6**: 233–291.

Grodzicki, A., 1998. Litostratigraphy, petrography and mineralogy of Cainozoic gold-bearing sands from Lower Silesia (in Polish with English summary). Physicochemical Problems of Mineral Processing, **32**: 31–41.

Grodzicki, A. 2011. Placer gold in Sudetes Mountains and in their foreland. Archivum Mineralogiae Monograph, **2**: 191–208.

Janeczek, J., 1985. Typomophic minerals of pegmatites from the Strzegom-Sobótka granitic massif. Geologia Sudetica, **20**: 1–63.

Jęczmyk, M., Krzemińska, E., 1996. Skład chemiczny złota okruchowego w utworach aluwialnych Pogórza Izerskiego (in Polish). Przegląd Geologiczny, **44**: 285–290.

Kania, M., 2018. Application of the chemical-mineralogical assays of placer gold grains in the prospection of the polymetallic mineralisation (in Polish with English summary). Górnictwo Odkrywkowe, **3**: 115–122.

Kania, M., 2020. Detrital gold origin research methodology (in Polish with English summary). Górnictwo Odkrywkowe, **4**: 25–34.

Kania, M., 2023. Chemical and mineralogical characteristics and origin of placer gold from fluvial deposits of Żeliszowski Creek (North Sudetic Basin, SW Poland). Geological Quarterly, **67**, 12; https://doi.org/10.7306/gq.1682

Kania, M., Muszer, A., 2024. The Skora River: an anthropogenically modified gold-bearing fluvial deposit (North Sudetic Trough, SW Poland). Geological Quarterly, **68**, 35; https://doi.org/10.7306/gq.1763

Kossowska, I., 1975. Ocena występowania kaolinów na obszarze masywów metamorficznych. Badania mineralogiczne skaolinizowanych skał krystalicznych z przedpola Gór Sowich i Wądroża Wielkiego (in Polish). Centralne Archiwum Geologiczne PIG-PIB, Oddział Dolnośląski, Wrocław (nr inw. 4422/153).

Kozdrój, W., 2009. Szczegółowa Mapa Geologiczna Polski, 1:50 000, arkusz 797 – Bolków (in Polish). Państw. Inst. Geol. – PIB, Warszawa.

Kozdrój, W., Ihnatowicz, A., Przybylski, B., 2012. Szczegółowa Mapa Geologiczna Polski, 1:50 000, arkusz 759 – Złotoryja (in Polish). Państw. Inst. Geol. – PIB, Warszawa.

Kozłowska-Koch, M., 1959. Granitognejsy Wądroża Wielkiego (in Polish). Archiwum Mineralogiczne, **21**: 383–408.

Kozłowski, A., 2011. Native gold in quartz pebbles of the Baltic shore, West Pomerania. Archivum Mineralogiae Monograph, **2**: 353–367.

Kryza, R., Muszyński, A., 2003. Kompleks metamorficzny Gór Kaczawskich - fragment waryscyjskiej pryzmy akrecyjnej (in Polish). In: Sudety zachodnie: od wendu do czwartorzędu (ed. A. Ciężkowski, J. Wojewoda and A. Żelaźniewicz): 95–105. WIND, Wrocław.

Kural, S., Jerzmański, J., 1974. Objaśnienia do Szczegółowej mapy Sudetów, arkusz Goczałków (in Polish). Wydaw. Geol., Warszawa.

Leake, R.C., Styles, M.T., Bland, D.J., Henney, P.J., Wetton, P.D., Naden, J., 1995. The interpretation of alluvial gold characteristics as an exploration technique. British Geological Survey, ODA Technical Report WC/95/22, Overseas Geology Series. Keyworth, Nottingham.

Maciejak, K., 2011a. Górnictwo złota w Górach Kaczawskich i na ich przedpolu (in Polish). Archivum Mineralogiae Monograph, **2**: 243–294.

Maciejak, K., 2011b. Gold mining in the Kaczawa Mountains and in the surrounding area – a review. Archivum Mineralogiae Monograph, **2**: 295–304.

Majerowicz, A., 1963. The granite of the environs of Sobótka and its relation to the country rocks (in Polish with English summary). Archiwum Mineralogiczne, **24**: 127–227.

Mazur, S., Aleksandrowski, P., Kryza, R., Oberc-Dziedzic, T., 2006. The Variscan Orogen in Poland. Geological Quarterly, **50** (1): 89–118.

Mikulski, S.Z., 2007. The late Variscan gold mineralization in the Kaczawa Mountains, Western Sudetes. Polish Geological Institute Special Papers, **22**: 1–162.

Mikulski, S.Z., 2011. Gold deposits in Kaczawa Mountains, West Sudetes, SW Poland. Archivum Mineralogiae Monograph, **2**: 63–83.

Mikulski, S.Z., Ostrowski, S., 2023. Geochemical, mineralogical and geophysical studies (VLF) in the prospecting for vein-type gold deposits in the former Klecza-Radomice Ore District in the Kaczawskie Mountains (in Polish with English summary). Przegląd Geologiczny, **71**: 219–223; https://doi.org/10.7306/2023.17

Mikulski, S.Z., Wierchowiec, J., 2013. Placer scheelite and gold from alluvial sediments as indicators of primary mineralisation – examples from SW Poland. Geological Quarterly, **57** (3): 503–514; https://doi.org/10.7306/gq.1107

Muszer, A., Ćwiertnia, J., Kania, M., 2016. Anthropogenic gold from Złotoryja area (Kaczawa Foothills) (in Polish with English summary). Górnictwo Odkrywkowe, **4**: 5–11.

Paulo, A., 1970. Nickel and bismuth minerals in ore veins in the environs of Chełmiec (Kaczawa Mts., Lower Silesia) (in Polish with English summary). Prace Mineralogiczne, **24**: 61–77.

Pin, C., Puziewicz, J., Duthou, J.L., 1989. Ages and origis of a composite granitic massif in the Variscan belt: a Rb-Sr study of the Strzegom-Sobótka massif, W Sudetes (Poland). Neues Jahrbuch für Mineralogie Abhandlungen, **160**: 71–82.

Pitfield, P.E.J., Styles, M.T., Taylor, C.D., Key, R.M., Vonimanitra Ralison, A., 2009. Gold deposit styles and placer gold chracteristaion in northern and east-central Madagascar. In: Smart science for exploration and mining: Proceedings of the 10th Biennial SGA Meeting, Townsville, Australia, August 17th–20th.

Przybylski, B., 2009. Szczegółowa Mapa Geologiczna Polski, 1:50 000, arkusz 798 – Świdnica (in Polish). Państw. Inst. Geol. – PIB, Warszawa.

Styles, M.T., 1995. Alluvial gold characterization in exploration planning: project summary report. British Geological Survey, ODA Technical Report WC/95/38, Overseas Geology Series. Keyworth, Nottingham.

Szamałek, K., Szuflicki, M., Mizerski, W. (ed.), 2020. Bilans perspektywicznych zasobów kopalin Polski wg stanu na 31.12.2018 r. (in Polish). Państw. Inst. Geol. – PIB, Warszawa.

Townley, B.K., Hérail, G., Maksaev, V., Palacios, C., de Parseval, P., Sepulveda, F., Orellana, R., Rivas, P., Ulloa, C., 2003. Gold grain morphology and composition as an exploration tool: application to gold exploration in covered areas. Geochemistry: Exploration, Environment, Analysis, **3**: 29–38; https://doi.org/10.1144/1467-787302-042

Uberna, J., 1959. Kaolin i żyły kwarcowe w rejonie Wądroża Wielkiego (in Polish). Przegląd Geologiczny, **7**: 536–537.

Urbański, K., 2009a. Szczegółowa Mapa Geologiczna Polski, 1:50 000, arkusz 760 – Jawor (in Polish). Państw. Inst. Geol. – PIB, Warszawa.

Urbański, K., 2009b. Szczegółowa Mapa Geologiczna Polski, 1:50 000, arkusz 761 – Wądroże Wielkie (in Polish). Państw. Inst. Geol. – PIB, Warszawa.

Urbański, K., Różański, P., 2016. Objaśnienia do Szczegółowej Mapy Geologicznej Polski 1:50 000. Arkusz Wądroże Wielkie (761) (in Polish). Państw. Inst. Geol. – PIB, Warszawa.

Wierchowiec, J., 2010. Gold in technogenous placers of Lower Silesia, Poland. Warsaw University Press.

Wierchowiec J., Zieliński, K., 2017. Origin of placer gold and other heavy minerals from fluvial Cenozoic sediments in close proximity to Rote Fäule-related Au mineralisation in the North Sudetic Trough, SW Poland. Geological Quarterly, **61** (1): 62–80; https://doi.org/10.7306/gq.1315

Wierchowiec, J., Mikulski, S.Z., Gąsiński, A., 2018. Nanoforms of gold from abandoned placer deposits of Wądroże Wielkie, Lower Silesia, Poland – The evidence of authigenic gold mineralization. Ore Geology Reviews, **101**: 211–220; https://doi.org/10.1016/j.oregeorev.2018.07.009

Wołkowicz, K., 2015. Accessory minerals in the quartz rock from the Wądroże Wielkie area (Fore-Sudetic Block) – preliminary data (in Polish with English summary). Biuletyn Państwowego Instytutu Geologicznego, **464**: 79–90; https://doi.org/10.5604/08676143.1200435

Yushko-Zakharova, O.E., Ivanov, V.V., Soboleva, L.N. (ed.),1986. Minerali blagorodnyhh metallov (in Russian). Nedra, Moskva.

Zöller, A., Heuseler, E., 1926. Die Goldquarzgänge und Goldseifen zwischen Grosswandriss und Wahlstatt in Niederschlesien. Glückauf, **48**: 1585–1588.

Żelaźniewicz, A., 1997. The Sudetes as Palaeozoic orogen in central Europe. Geological Magazine, **134**: 691–702; https://doi.org/10.1017/S0016756897007541

Żelaźniewicz, A., 2003. Postęp wiedzy o geologii krystaliniku Sudetów w latach 1990–2003 (in Polish). In: Sudety Zachodnie: od wendu do czwartorzędu (ed. W. Ciężkowski, W., Wojewoda and J. Żelaźniewicz): 7–16. WIND, Wrocław.

Żelaźniewicz, A., Cwojdziński, S., England, W.R., Zientara, P., 1997. Variscides in the Sudetes and the reworked Cadomian orogen: evidence from the GB-2A seismic profiling in the southwestern Poland. Geological Quarterly, **41** (3): 289–308.

Żelaźniewicz, A., Dorr, W., Bylina, P., Franke, W., Haack, U., Heinisch, H., Schastok, J., Grandmontagne, K., Kulicki, C., 2004. The eastern continuation of the Cadomian orogen: U-Pb zircon evidence from Saxo-Thuringian granitoids in south-western Poland and the northern Czech Republic. International Journal of Earth Sciences, **93**: 773–781; https://doi.org/10.1007/s00531-004-0418-3

Żelaźniewicz, A., Aleksandrowski, P., 2008. Tectonic subdivision of Poland: southwestern Poland (in Polish with English summary). Przegląd Geologiczny, **56**: 904–911.

Żelaźniewicz, A., Aleksandrowski, P., Buła, Z., Karnkowski, P.H., Konon, A., Oszczypko, N., Ślączka, A., Żaba, J., Żytko, K., 2011. Regionalizacja tektoniczna Polski (in Polish). Komitet Nauk Geologicznych PAN, Wrocław.

APPENDIX 1

Characteristic EDS spectra and elemental compositions of the micro-inclusions and the Ag contents in gold grains from the Wierzbiak channel-fill deposits

For the EDS analyses, the polished sections containing gold grains were coated with graphite. Each analytical session was preceded by calibration (Energy-Channel Calibration / Energy-Axis Calibration), in accordance with the recommendations of Bruker, the manufacturer of the EDS detectors and analytical software. Calibration was performed using a copper standard, due to significant differences in critical ionization energies between the K, L and M lines, which ensures more precise comparison between analysed and theoretical spectra.

The analyses were applied in high vacuum conditions, with the electron beam acceleration voltage of 25 keV and beam current of 15 nA. The characteristic X-ray spectra obtained were processed using Bruker Esprit v1.9 software. Point analyses were preceded by surface elemental mapping of the following elements: Ag, As, Au, Bi, Cd, Co, Cr, Cu, Fe, Hg, Ir, Mn, Mo, Ni, Os, Pb, Pd, Pt, Rh, Ru, S, Sb, Se, Si, Sn, Te, Ti, V, W, Zn. This procedure minimized the risk of the overlooking finer microinclusions (< 1 μm in diameter), which can be missed during observations in reflected light. The gold grains selected, with a complex Au-Ag phase composition of Au-Ag, were also examined by linear analyses.

A total of 60 spot analyses, 9 line analyses, and 280 surface analyses were performed on the research material. Acquisition times of the EDS analyses were set to 60 s (point analyses), 90 s (linear analyses) and 120 s (elemental mapping). The extended acquisition times allowed generating spectra based on over a million counts for a single spectrum, enhancing the credibility of results of the semi-quantitative analyses. Quantification of the data was carried out using the PB-ZAF correction procedure, including Carbon Correction to account the graphite coating.

Each spectrum obtained was interpreted manually with particular attention paid to artefactual peaks (especially summary ones), which frequently formed in the 4.5–5.0 keV range as an effect of the strong Au M peak creation. Bremsstrahlung background shapes were also fitted manually. During interpretation, a built-in deconvolution tool was used to compare theoretical spectra as a composition of a selected set of elements with the actual characteristic spectra. This approach enabled accurate identification of overlaps of the elements and evaluation of elemental composition of the sample by eliminating false positives or incorporating previously undetected elements. A detection threshold of 0.1 wt.% was adopted for each element. Characteristic EDS spectra and elemental compositions of the Au-Ag alloys and microinclusions identified in gold grains collected from the Wierzbiak River channel-fill deposits are shown below:

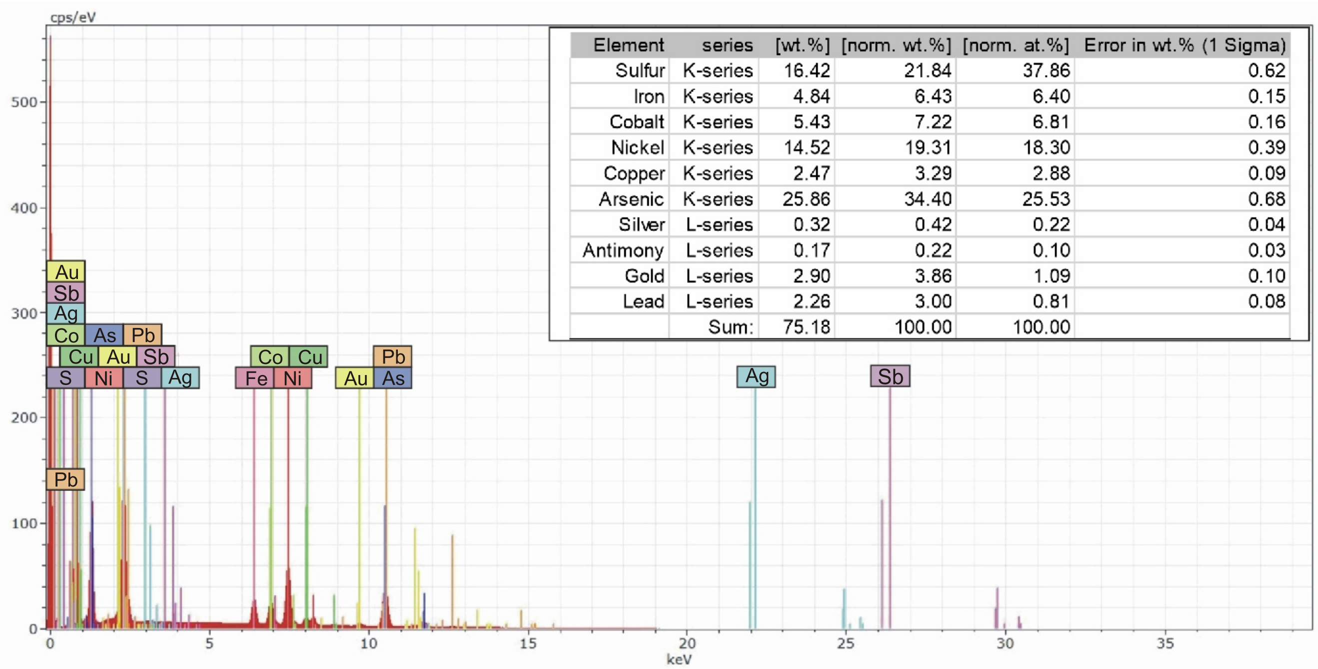

Element	series	[wt.%]	[norm. wt.%]	[norm. at.%]	Error in wt.% (1 Sigma)
Sulfur	K-series	16.42	21.84	37.86	0.62
Iron	K-series	4.84	6.43	6.40	0.15
Cobalt	K-series	5.43	7.22	6.81	0.16
Nickel	K-series	14.52	19.31	18.30	0.39
Copper	K-series	2.47	3.29	2.88	0.09
Arsenic	K-series	25.86	34.40	25.53	0.68
Silver	L-series	0.32	0.42	0.22	0.04
Antimony	L-series	0.17	0.22	0.10	0.03
Gold	L-series	2.90	3.86	1.09	0.10
Lead	L-series	2.26	3.00	0.81	0.08
	Sum:	75.18	100.00	100.00	

Fig. I. X-ray spectrum and point analysis results W-6.I – Ni-Co-Fe sulpharsenide within the W-6 gold grain

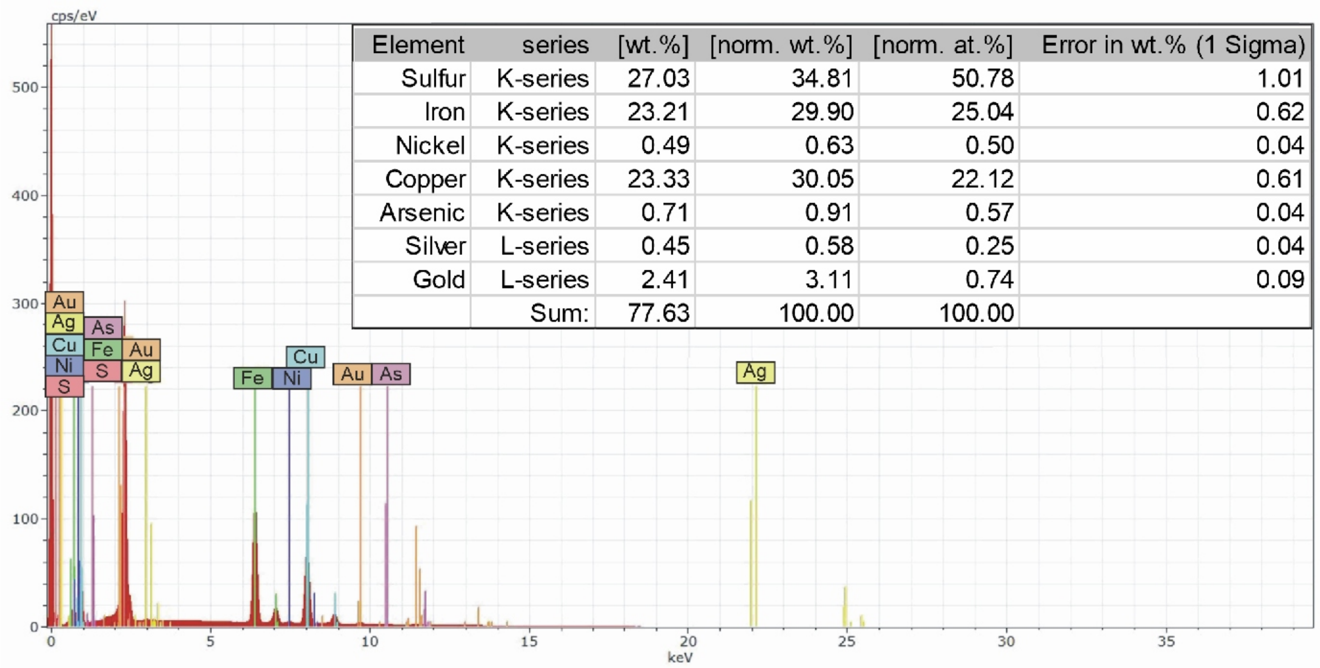

Element	series	[wt.%]	[norm. wt.%]	[norm. at.%]	Error in wt.% (1 Sigma)
Sulfur	K-series	27.03	34.81	50.78	1.01
Iron	K-series	23.21	29.90	25.04	0.62
Nickel	K-series	0.49	0.63	0.50	0.04
Copper	K-series	23.33	30.05	22.12	0.61
Arsenic	K-series	0.71	0.91	0.57	0.04
Silver	L-series	0.45	0.58	0.25	0.04
Gold	L-series	2.41	3.11	0.74	0.09
	Sum:	77.63	100.00	100.00	

Fig. II. X-ray spectrum and point analysis results W-6.II – Cu sulphide with an elemental composition similar to chalcopyrite within the W-6 gold grain

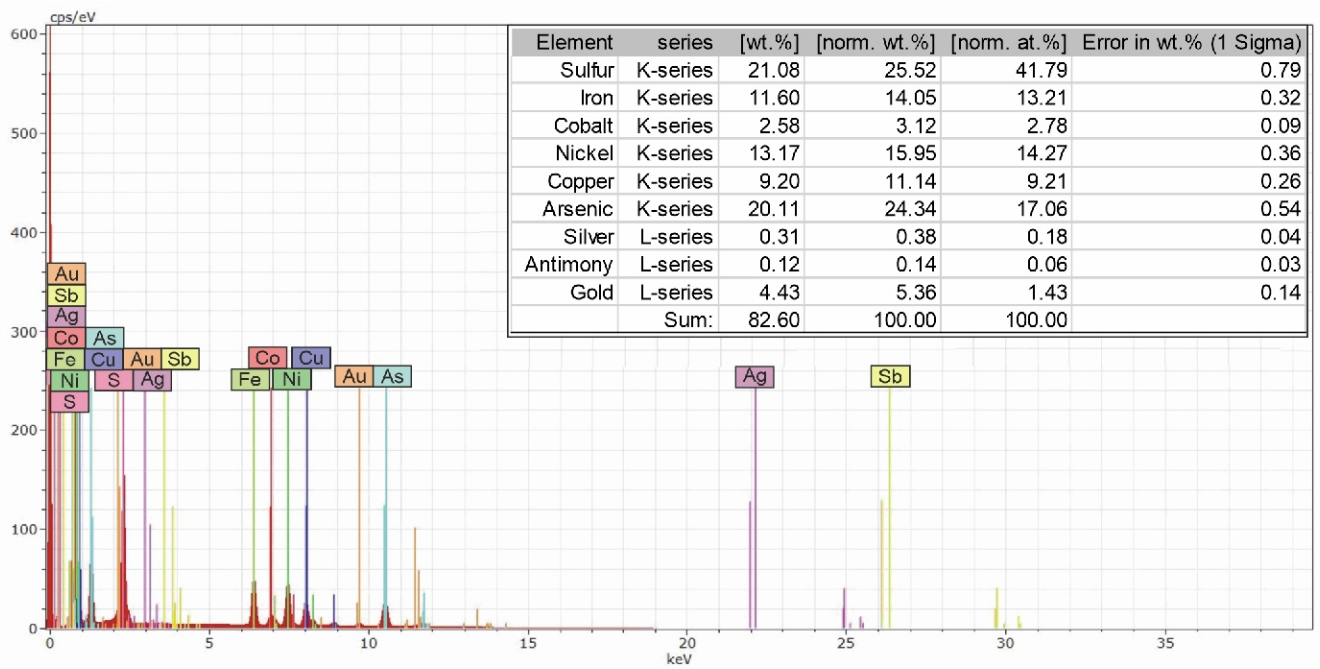

Element	series	[wt.%]	[norm. wt.%]	[norm. at.%]	Error in wt.% (1 Sigma)
Sulfur	K-series	21.08	25.52	41.79	0.79
Iron	K-series	11.60	14.05	13.21	0.32
Cobalt	K-series	2.58	3.12	2.78	0.09
Nickel	K-series	13.17	15.95	14.27	0.36
Copper	K-series	9.20	11.14	9.21	0.26
Arsenic	K-series	20.11	24.34	17.06	0.54
Silver	L-series	0.31	0.38	0.18	0.04
Antimony	L-series	0.12	0.14	0.06	0.03
Gold	L-series	4.43	5.36	1.43	0.14
	Sum:	82.60	100.00	100.00	

Fig. III. X-ray spectrum and point analysis results W-6.III – Ni-Fe-Co sulpharsenide within the W-6 gold grain

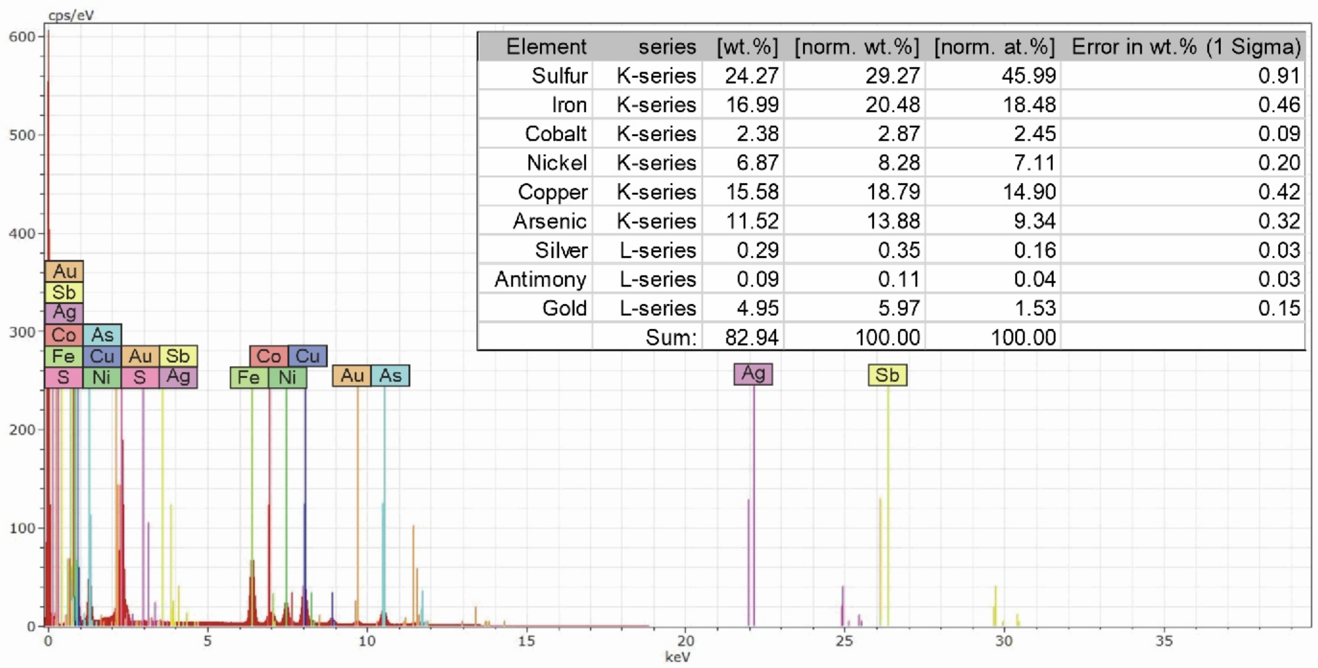

Element	series	[wt.%]	[norm. wt.%]	[norm. at.%]	Error in wt.% (1 Sigma)
Sulfur	K-series	24.27	29.27	45.99	0.91
Iron	K-series	16.99	20.48	18.48	0.46
Cobalt	K-series	2.38	2.87	2.45	0.09
Nickel	K-series	6.87	8.28	7.11	0.20
Copper	K-series	15.58	18.79	14.90	0.42
Arsenic	K-series	11.52	13.88	9.34	0.32
Silver	L-series	0.29	0.35	0.16	0.03
Antimony	L-series	0.09	0.11	0.04	0.03
Gold	L-series	4.95	5.97	1.53	0.15
	Sum:	82.94	100.00	100.00	

Fig. IV. X-ray spectrum and point analysis results W-6.IV – Fe-Ni-Co sulpharsenide within the W-6 gold grain

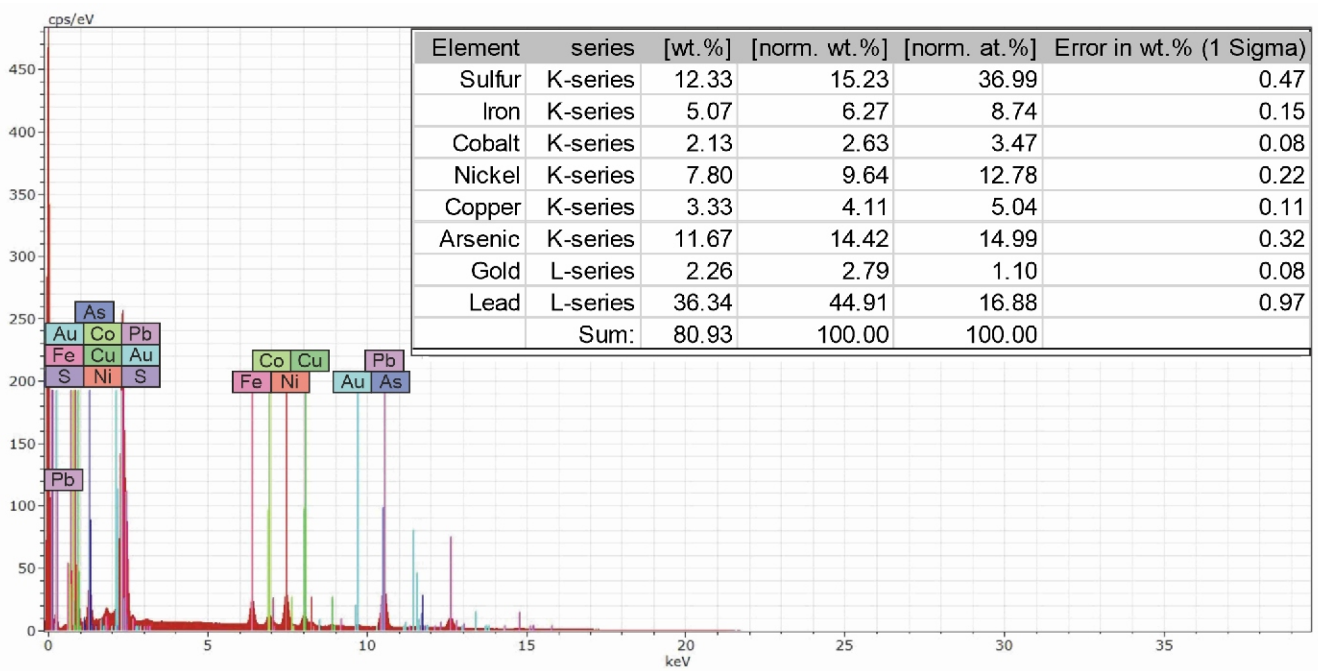

Element	series	[wt.%]	[norm. wt.%]	[norm. at.%]	Error in wt.% (1 Sigma)
Sulfur	K-series	12.33	15.23	36.99	0.47
Iron	K-series	5.07	6.27	8.74	0.15
Cobalt	K-series	2.13	2.63	3.47	0.08
Nickel	K-series	7.80	9.64	12.78	0.22
Copper	K-series	3.33	4.11	5.04	0.11
Arsenic	K-series	11.67	14.42	14.99	0.32
Gold	L-series	2.26	2.79	1.10	0.08
Lead	L-series	36.34	44.91	16.88	0.97
	Sum:	80.93	100.00	100.00	

Fig. V. X-ray spectrum and point analysis results W-6.V – Pb sulphide with an elemental composition similar to galena within the W-6 gold grain

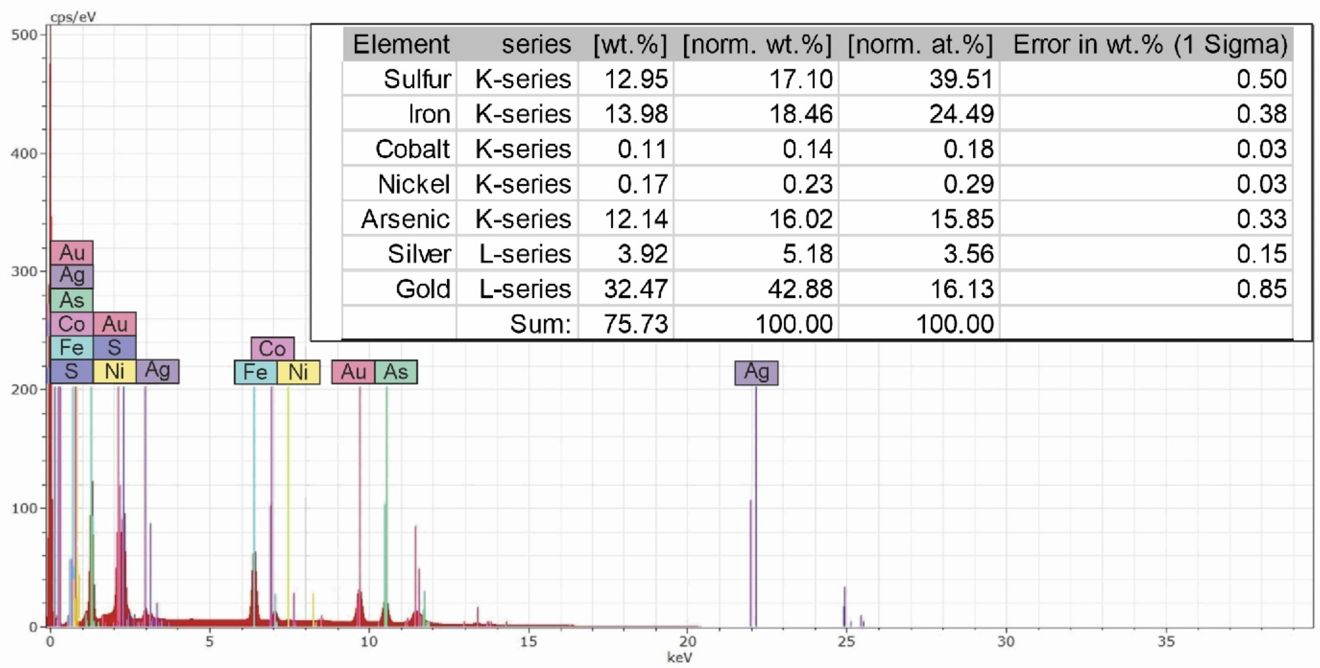

Element	series	[wt.%]	[norm. wt.%]	[norm. at.%]	Error in wt.% (1 Sigma)
Sulfur	K-series	12.95	17.10	39.51	0.50
Iron	K-series	13.98	18.46	24.49	0.38
Cobalt	K-series	0.11	0.14	0.18	0.03
Nickel	K-series	0.17	0.23	0.29	0.03
Arsenic	K-series	12.14	16.02	15.85	0.33
Silver	L-series	3.92	5.18	3.56	0.15
Gold	L-series	32.47	42.88	16.13	0.85
	Sum:	75.73	100.00	100.00	

Fig. VI. X-ray spectrum and point analysis results W-6.VI – Fe sulpharsenide with an elemental composition similar to arsenopyrite within the W-6 gold grain

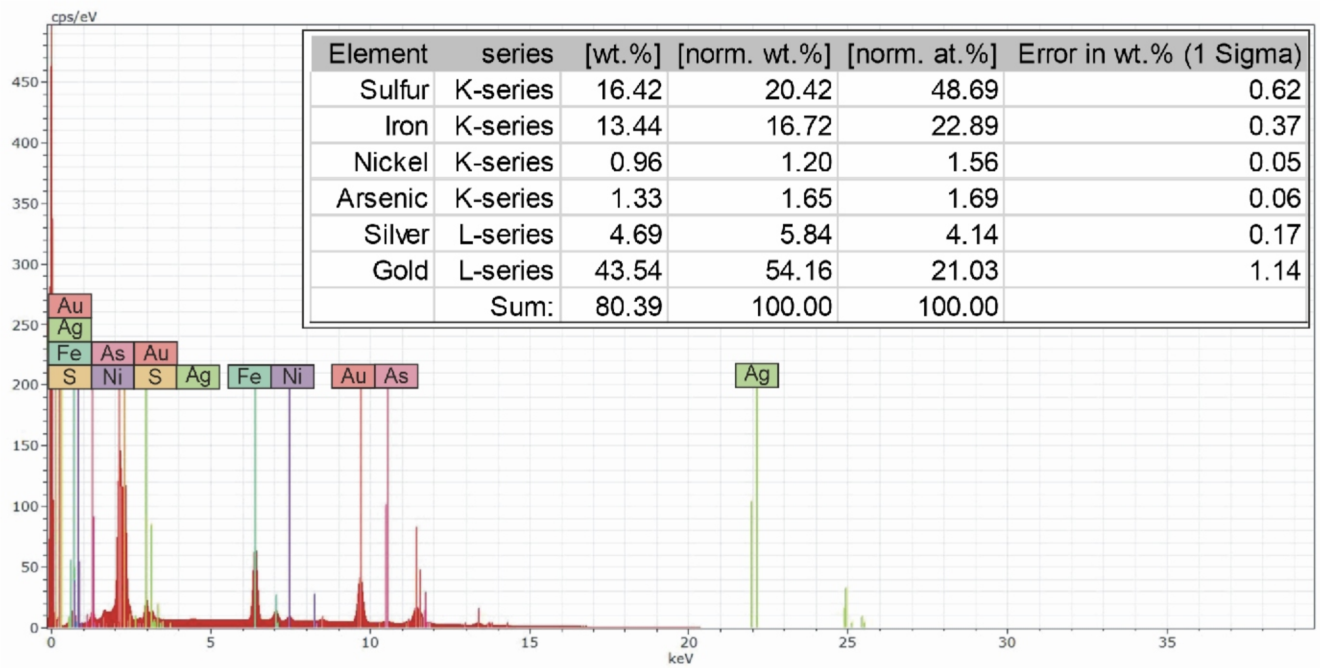

Element	series	[wt.%]	[norm. wt.%]	[norm. at.%]	Error in wt.% (1 Sigma)
Sulfur	K-series	16.42	20.42	48.69	0.62
Iron	K-series	13.44	16.72	22.89	0.37
Nickel	K-series	0.96	1.20	1.56	0.05
Arsenic	K-series	1.33	1.65	1.69	0.06
Silver	L-series	4.69	5.84	4.14	0.17
Gold	L-series	43.54	54.16	21.03	1.14
	Sum:	80.39	100.00	100.00	

Fig. VII. X-ray spectrum and point analysis results W-6.VII – Fe sulphide with an elemental composition similar to pyrite within the W-6 gold grain

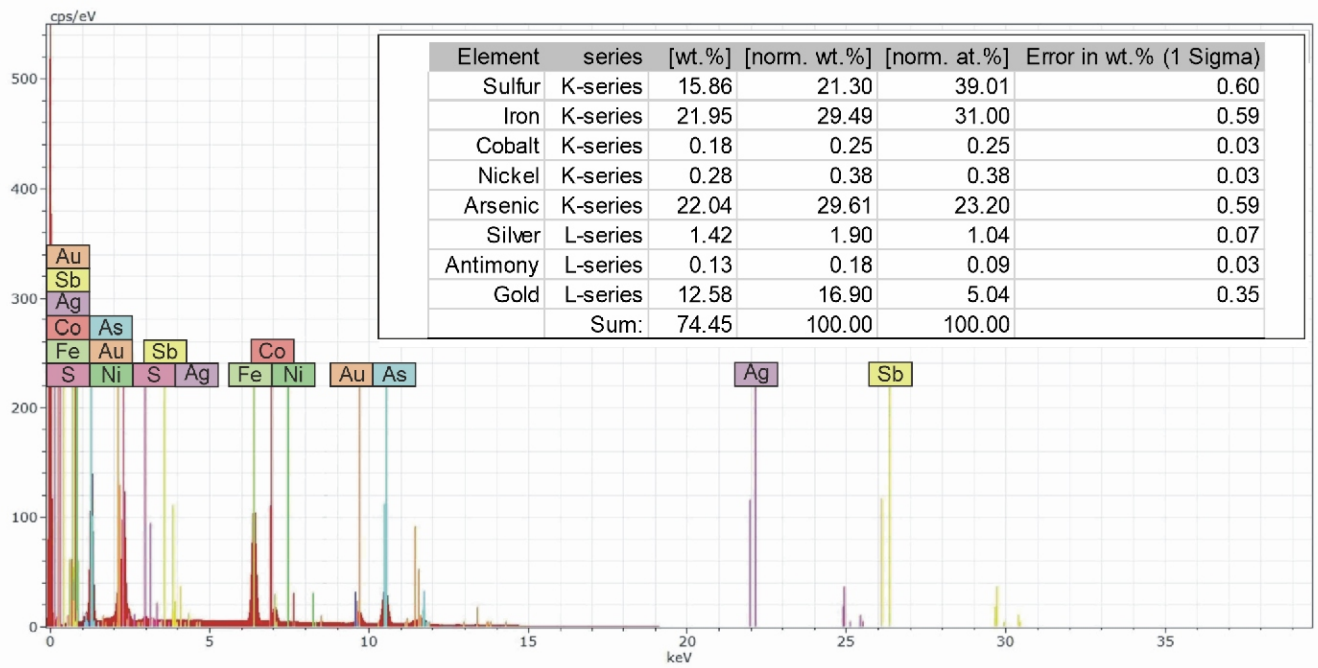

Element	series	[wt.%]	[norm. wt.%]	[norm. at.%]	Error in wt.% (1 Sigma)
Sulfur	K-series	15.86	21.30	39.01	0.60
Iron	K-series	21.95	29.49	31.00	0.59
Cobalt	K-series	0.18	0.25	0.25	0.03
Nickel	K-series	0.28	0.38	0.38	0.03
Arsenic	K-series	22.04	29.61	23.20	0.59
Silver	L-series	1.42	1.90	1.04	0.07
Antimony	L-series	0.13	0.18	0.09	0.03
Gold	L-series	12.58	16.90	5.04	0.35
	Sum:	74.45	100.00	100.00	

Fig. VIII. X-ray spectrum and point analysis results W-6.VIII – Fe sulpharsenide with an elemental composition similar to arsenopyrite within the W-6 gold grain

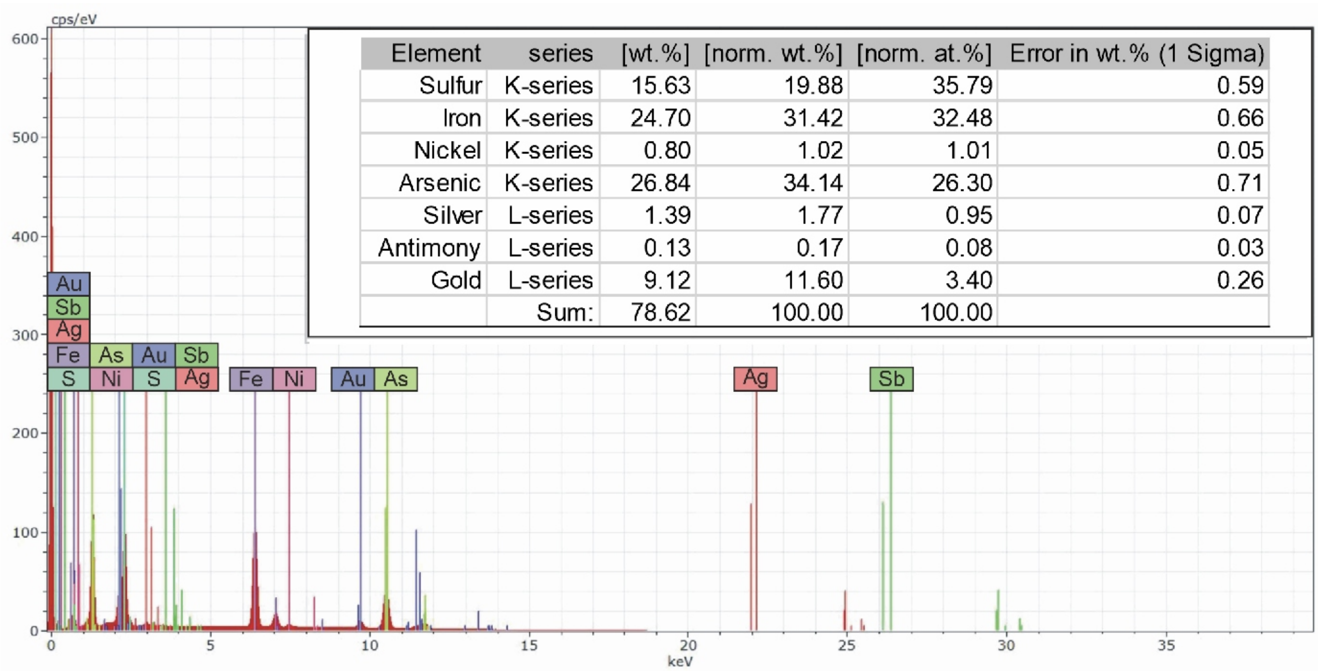

Element	series	[wt.%]	[norm. wt.%]	[norm. at.%]	Error in wt.% (1 Sigma)
Sulfur	K-series	15.63	19.88	35.79	0.59
Iron	K-series	24.70	31.42	32.48	0.66
Nickel	K-series	0.80	1.02	1.01	0.05
Arsenic	K-series	26.84	34.14	26.30	0.71
Silver	L-series	1.39	1.77	0.95	0.07
Antimony	L-series	0.13	0.17	0.08	0.03
Gold	L-series	9.12	11.60	3.40	0.26
	Sum:	78.62	100.00	100.00	

Fig. IX. X-ray spectrum and point analysis results W-6.IX – Fe sulpharsenide with an elemental composition similar to arsenopyrite within the W-6 gold grain

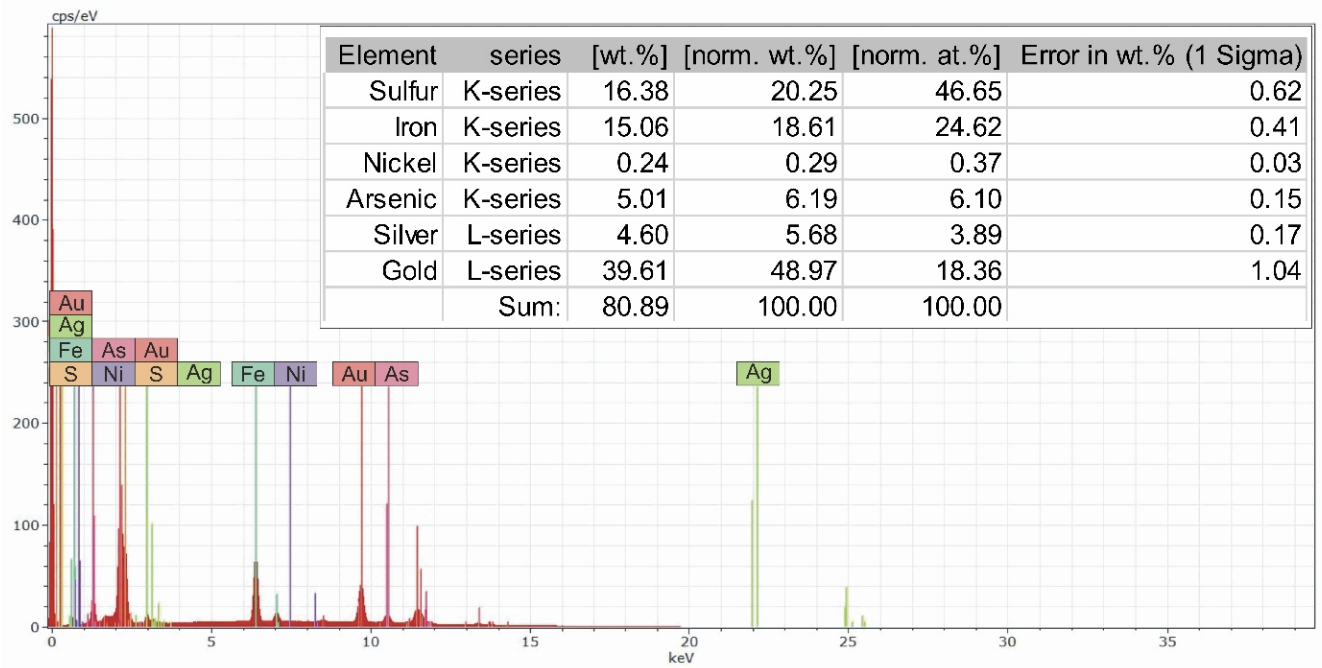

Element	series	[wt.%]	[norm. wt.%]	[norm. at.%]	Error in wt.% (1 Sigma)
Sulfur	K-series	16.38	20.25	46.65	0.62
Iron	K-series	15.06	18.61	24.62	0.41
Nickel	K-series	0.24	0.29	0.37	0.03
Arsenic	K-series	5.01	6.19	6.10	0.15
Silver	L-series	4.60	5.68	3.89	0.17
Gold	L-series	39.61	48.97	18.36	1.04
	Sum:	80.89	100.00	100.00	

Fig. X. X-ray spectrum and point analysis results W-6.X – Fe sulphide with the elemental composition similar to pyrite within the W-6 gold grain

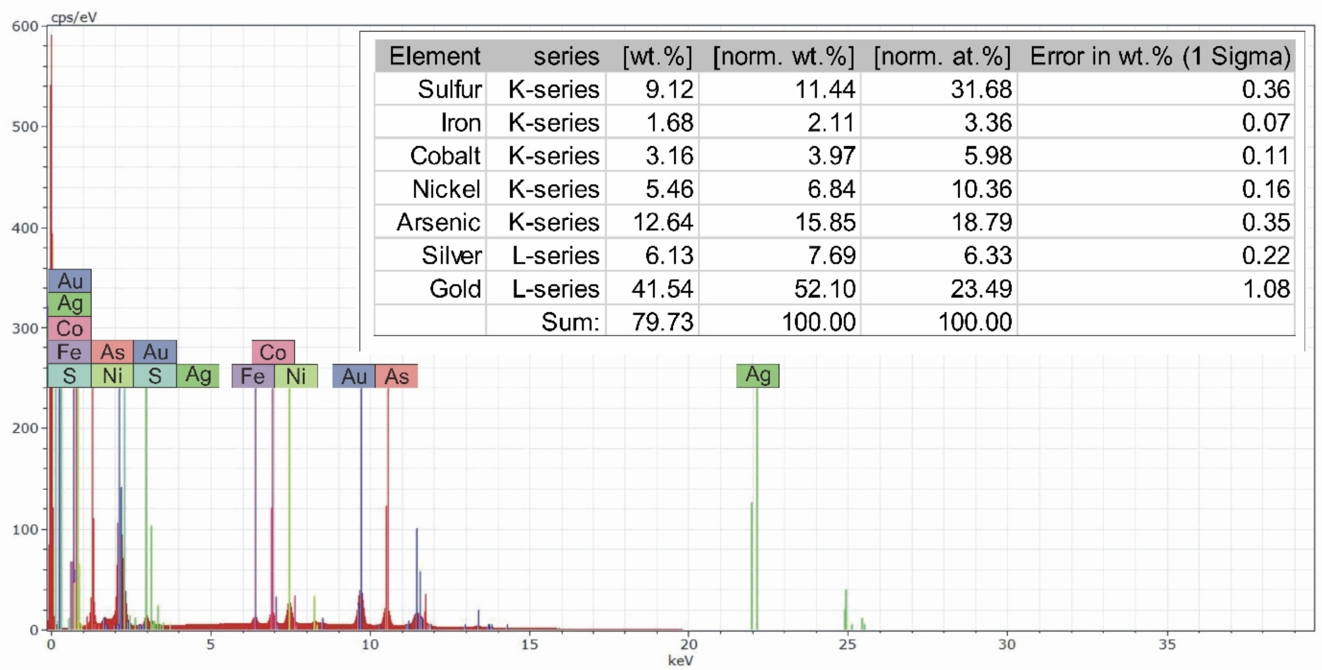

Element	series	[wt.%]	[norm. wt.%]	[norm. at.%]	Error in wt.% (1 Sigma)
Sulfur	K-series	9.12	11.44	31.68	0.36
Iron	K-series	1.68	2.11	3.36	0.07
Cobalt	K-series	3.16	3.97	5.98	0.11
Nickel	K-series	5.46	6.84	10.36	0.16
Arsenic	K-series	12.64	15.85	18.79	0.35
Silver	L-series	6.13	7.69	6.33	0.22
Gold	L-series	41.54	52.10	23.49	1.08
	Sum:	79.73	100.00	100.00	

Fig. XI. X-ray spectrum and point analysis results W-6.XI – Ni-Co-Fe sulpharsenide within the W-6 gold grain

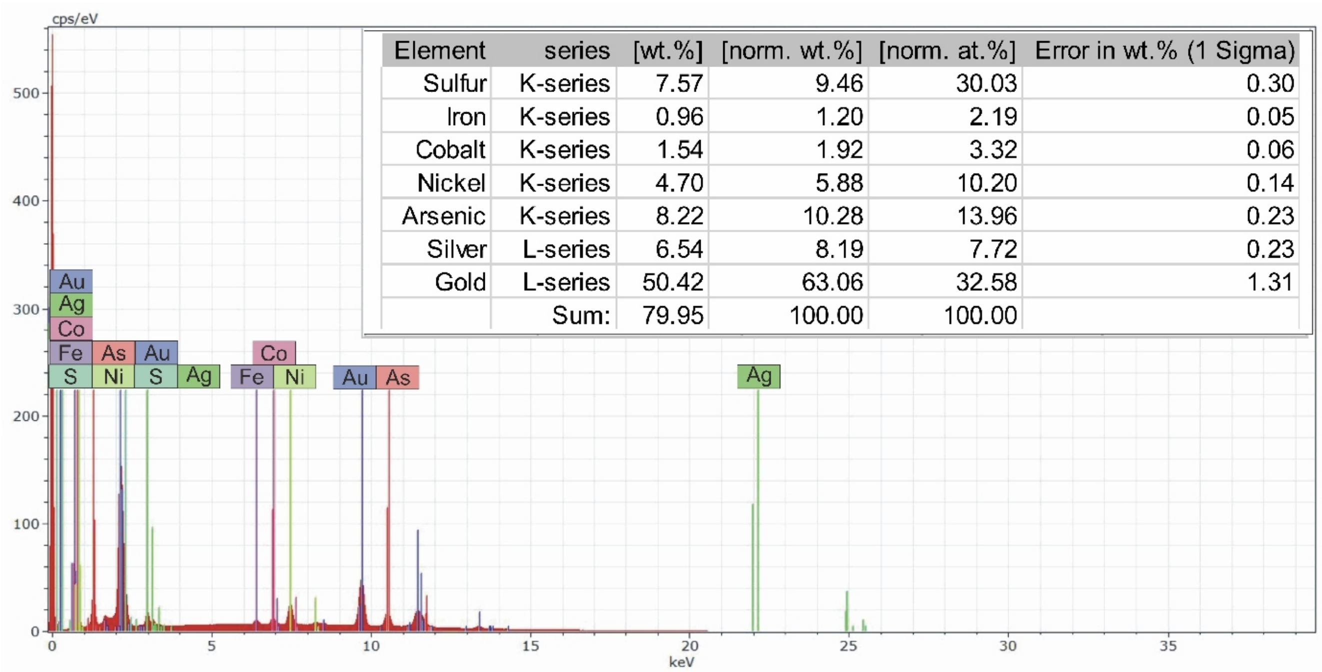

Element	series	[wt.%]	[norm. wt.%]	[norm. at.%]	Error in wt.% (1 Sigma)
Sulfur	K-series	7.57	9.46	30.03	0.30
Iron	K-series	0.96	1.20	2.19	0.05
Cobalt	K-series	1.54	1.92	3.32	0.06
Nickel	K-series	4.70	5.88	10.20	0.14
Arsenic	K-series	8.22	10.28	13.96	0.23
Silver	L-series	6.54	8.19	7.72	0.23
Gold	L-series	50.42	63.06	32.58	1.31
	Sum:	79.95	100.00	100.00	

Fig. XII. X-ray spectrum and point analysis results W-6.XII – Ni-Co-Fe sulpharsenide within the W-6 gold grain

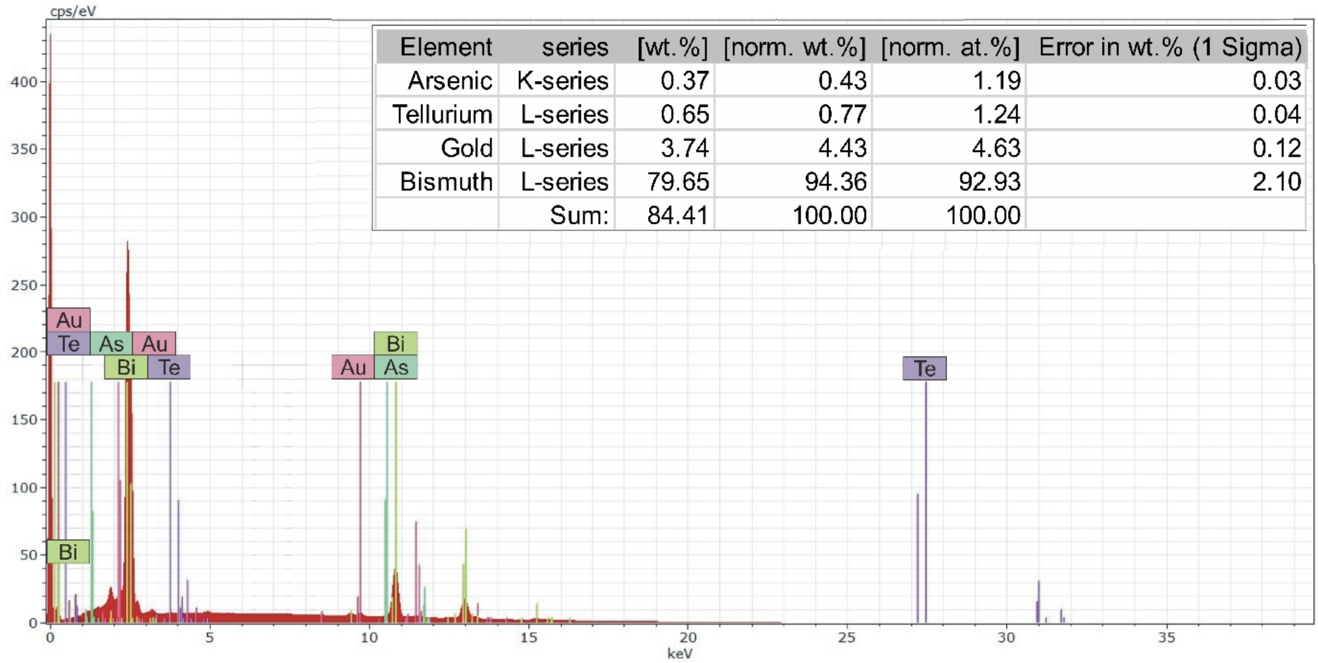

Element	series	[wt.%]	[norm. wt.%]	[norm. at.%]	Error in wt.% (1 Sigma)
Arsenic	K-series	0.37	0.43	1.19	0.03
Tellurium	L-series	0.65	0.77	1.24	0.04
Gold	L-series	3.74	4.43	4.63	0.12
Bismuth	L-series	79.65	94.36	92.93	2.10
	Sum:	84.41	100.00	100.00	

Fig. XIII. X-ray spectrum and point analysis results W-9.I – native bismuth within the W-9 gold grain

T a b l e I

Results of semi-quantitative analyses (wt.%) in polished sections of gold grain alloys

Grain	Point analysis	Ag (% wag.)
W-1	W-1.1	0.26
	W-1.2	11.34
	W-1.3	11.29
	W-1.4	0.00
	W-1.5	10.42
	W-1.6	0.32
	W-1.7	10.78
	W-1.8	11.21
W-2	W-2.1	2.95
	W-2.2	0.00
	W-2.3	1.62
W-3	W-3.1	15.64
	W-3.2	1.9
W-4	W-4.1	7.83
	W-4.2	0.00
	W-4.3	0.00
W-5	W-5.1	0.00
	W-5.2	10.83
	W-5.3	9.28
	W-5.4	9.48
W-6	W-6.1	16.18
	W-6.2	14.52
W-7	W-7.1	19.98
	W-7.2	9.32
	W-7.3	12.27
W-8	W-8.1	14.29
	W-8.2	14.14
	W-8.3	15.27
W-9	W-9.1	2.4
	W-9.2	2.76